IX.84.12607
63

NASA TECHNICAL MEMORANDUM

NASA TM X-873

NASA TM X-873

DECLASSIFIED- 1/31/68
AUTHORITY- TAINE TO SHAUKLAS
MEMO. US: 2840 dated 2/6/68

Declassified by authority of NASA
Classification Change Notices No. 137
Dated ** 2/14/68

FACILITY FORM 602
N68-83472 (ACCESSION NUMBER)
9 (PAGES)
(NASA CR OR TMX OR AD NUMBER)
(THRU)
(CODE)
(CATEGORY)

WEIGHTLESSNESS EXPERIMENTS WITH LIQUID HYDROGEN IN AEROBEE SOUNDING ROCKETS; NONUNIFORM RADIANT HEAT ADDITION-FLIGHT 4(U)

by John D. Regetz, Jr., Martin J. Conroy, and Robert G. Jackson

Lewis Research Center
Cleveland, Ohio

NATIONAL AERONAUTICS AND SPACE ADMINISTRATION • WASHINGTON, D. C. • FEBRUARY 1964

CONFIDENTIAL

WEIGHTLESSNESS EXPERIMENTS WITH LIQUID HYDROGEN IN AEROBEE SOUNDING ROCKETS; NONUNIFORM RADIANT HEAT ADDITION - FLIGHT 4

By John D. Regetz, Jr., Martin J. Conroy, and Robert G. Jackson

Lewis Research Center
Cleveland, Ohio

GROUP 4
Downgraded at 3 year intervals; declassified after 12 years

CLASSIFIED DOCUMENT—TITLE UNCLASSIFIED

This material contains information affecting the national defense of the United States within the meaning of the espionage laws, Title 18, U.S.C. Secs. 793 and 794, the transmission or revelation of which in any manner to an unauthorized person is prohibited by law.

NATIONAL AERONAUTICS AND SPACE ADMINISTRATION

CONFIDENTIAL

CONFIDENTIAL

WEIGHTLESSNESS EXPERIMENTS WITH LIQUID HYDROGEN IN AEROBEE SOUNDING ROCKETS; NONUNIFORM RADIANT HEAT ADDITION - FLIGHT 4*

By John D. Regetz, Jr., Martin J. Conroy, and Robert G. Jackson

Lewis Research Center

SUMMARY

A cryogenic heat-transfer experiment was conducted in a weightless environment for a period of about $3\frac{1}{2}$ minutes. The primary objective was to determine the fluid configuration and motion under conditions of weightlessness and low nonuniform radiant heating.

The experiment consisted of a spherical thin-walled hydrogen container, 25.1 percent filled with liquid hydrogen, surrounded by a nonuniform radiant heater. The outer surface of the hydrogen tank was instrumented with transducers that measured the temperature of the hydrogen at the wall and thus provided a means of determining whether the wall was liquid or vapor wetted.

Data indicate that, for about one-half the flight, the entire tank wall was liquid wetted. In addition, there appeared to be some fluid motion in the tank for an extensive period of time after all vehicle accelerations had ceased. At 180 seconds after rocket lift-off, the forward portion of the hydrogen container started to dry off. The vapor-covered area increased during the remainder of the flight and tended to increase faster toward the side of the tank subjected to the highest heating rates.

The wall temperatures show that the liquid adjacent to the wall was near the saturation temperature determined by the sphere pressure on the side having the lower heating rate, and an average temperature difference of about 1.5° R was established between that side and the warm side. This temperature difference remained essentially constant throughout the flight. Photographs show nucleate boiling and bubble motion during the later part of weightlessness. These data indicate the probability of fluid motion being induced by the momentum generated by bubble formation. The hydrogen pressure tended to rise faster than that which would be calculated by assuming a uniform bulk temperature for the liquid, which indicates that some of the liquid was subcooled.

*Title, Unclassified.

[redacted]

INTRODUCTION

The use of cryogenic liquids as propellants and coolants in space vehicles and systems has become firmly established. As part of the overall missions planned, it will be necessary for partially filled tanks containing these fluids to exist for extensive periods of time outside the Earth's atmosphere, where they will be subjected simultaneously to radiant heating from the sun and the albedos of the Earth and moon as well as to the phenomenon of zero gravity or weightlessness. Since radiant heat transfer into the fluid can cause propellant losses, the behavior of the liquid when heated in a weightless state must be known. Such behavior cannot always be predicted on the basis of standard 1-g ground tests, since the gravitational forces produce such effects as buoyancy and convection currents that are absent when gravity is removed (refs. 1 and 2).

Various methods have been devised for obtaining a weightless environment. Among these are drop towers, aircraft flying parabolic trajectories, and sounding rockets boosted into ballistic trajectories. The Lewis Research Center has conducted experiments utilizing all three types of facilities (refs. 3 and 4). Because of the much longer times required to conduct experiments involving the transfer of heat to the cryogenic liquid, the sounding rocket was chosen for this type of experiment. This facility has the capability of providing weightless periods of the order of minutes as compared with seconds from the other two types. This report describes one of a series of experiments on heat transfer in a weightless environment using an Aerobee 150A as the boost vehicle and liquid hydrogen as the cryogenic fluid. Previous experimental flights in this series are described in references 5 to 7. In these flights, liquid-hydrogen tanks having initial liquid fillings ranging from 22.5 to 34.3 percent were subjected to radiant heating rates ranging from 160 to 270 Btu per hour per square foot. The rocket vehicle and subsystems for this flight were identical to those of the third flight of the series (ref. 7). This experiment, however, differed from the previous one in the following respects: (1) The radiant heat was nonuniformly distributed around the liquid-hydrogen container, and (2) the overall heating rate was lower than on the previous flight. The experiment consisted of a spherical 9-inch-diameter stainless-steel tank that was 25.1 percent filled with hydrogen and was subjected to nonuniform radiant heating similar to that which a coasting space vehicle might be expected to receive from the sun. Instrumentation was included to measure vehicle performance, heat input to the hydrogen, hydrogen temperature, and hydrogen tank pressure. A motion picture camera was used to obtain photographs of the liquid hydrogen during the weightless portion of the trajectory.

The purpose of this experiment was to determine the fluid motion and configuration and the hydrogen pressure rise in the presence of nonuniform radiant heating and weightlessness.

APPARATUS

Vehicle Description

A sketch showing the major components of the Aerobee rocket and the payload

is presented in figure 1. The basic rocket was not changed. Various subsystems, however, were added to improve its performance as a zero-gravity facility. Since sustainer burnout occurs before the rocket leaves the sensible atmosphere, a drag force would ordinarily be exerted on the vehicle that might tend to induce undesirable motion in the liquid hydrogen at the start of the experimental period. To minimize this effect, residual pressurization gas from the oxidant tank was discharged from the rocket thrust nozzle for approximately 20 seconds after sustainer burnout. The thrust produced approximated the drag during this period and tended to negate its effects. At the end of this drag-cancellation period, residual fuel-tank gas was piped through two small nozzles arranged so as to despin the rocket engine casing. (The casing is spin-stabilized during engine burning.) The despin system was rate-gyro controlled so that the final casing spin rate was less than 2° per second. In addition, the payload was mounted on a rate-controlled, servomotor-driven turntable that separated it from the rocket casing. This turntable held the payload spin rate to less than 1° per second from lift-off throughout the flight. At the end of the weightless period, fuel-tank pressurization gas was piped through two small thrust nozzles in the rocket tail section to provide a collection thrust on the fluid.

Experiment Description

A cross-sectional sketch of the liquid-hydrogen tank is shown in figure 2. The inner sphere, containing the liquid hydrogen, was made of 0.010-inch-thick stainless steel. Sapphire windows were provided to accommodate a high-intensity light source and a 90° lens assembly for the movie camera. The outer structural sphere, 11 inches in diameter, was made of stainless steel and had cooling coils for liquid nitrogen wound on its outer surface. The fill and vent tube was designed to keep heat conduction from the outer sphere to the inner at a minimum. The hydrogen tank was suspended from the structural sphere by a polychlorotrifluoroethylene plastic ring, which had a number of cutouts to reduce heat conduction to the inner sphere. The outer surface of the hydrogen tank was instrumented with 19 small, flat platinum resistance temperature transducers; the leads of these transducers were attached to the exterior tank wall at several places and brought out through a small tube near the bottom of the tank to a connector mounted on a brass plate in the outer sphere. The space between inner and outer spheres was evacuated after assembly and maintained at a high vacuum.

The intermediate sphere, made of 0.016-inch copper and having a 10-inch diameter, acted as the heater sphere for the hydrogen tank. For the present experiment, the heater sphere was fabricated in four sections, segments of a sphere about the roll axis of the vehicle, as shown in figure 3. The 90° segment directly opposite the light source presented the maximum radiant heating rate to the hydrogen tank. During the experimental portion of the flight, this segment was controlled at such a design temperature as to give a nominal heating rate of 61.5 Btu per hour per square foot. The two 45° segments on either side of it were each held by controllers at a design temperature corresponding to a heating rate of 28 Btu per hour per square foot. Each of these three segments had a heating unit wound on its outer surface. Power to the units was turned on 39 seconds after launch, and the controllers were designed to bring the segments up to design temperature quickly with as little overshoot as possible.

The segments were maintained at about the desired temperature by applications of reduced power. The remaining half of the middle sphere was not directly heated, but was heated by conduction through the stainless-steel legs by which it was fastened to the outer structural sphere. Heat conduction through these legs caused the temperature of this hemisphere to approach that of the outer sphere. Each of these four segments was instrumented with platinum resistance transducers, and the temperatures measured were used to calculate the heat radiated to the hydrogen tank. A plot of the nominal heating rate against longitude angle produced by this configuration is given in figure 4.

The inner surface of the heater shell and the outer surface of the hydrogen tank were sprayed after instrumenting, before assembly, with approximately 0.002 inch of dull black lacquer to increase the emissivity of the surfaces.

Instrumentation Description

Telemetry and tracking. - Instrumentation and data signals were transmitted by PPM/AM telemetry to ground receiving stations located near the launch complex, where they were photographically recorded. Vehicle trajectory and velocity were determined by radar skin tracking.

Vehicle performance instrumentation. - Vehicle accelerations were sensed along each of three mutually perpendicular axes as follows: parallel to the rocket spin axis, by one -1 to +15 g, one ±0.5 g, two ±0.01 g accelerometers, and one 0.001 g accelerometer, and along each of the other two axes, pitch and yaw, by one ±0.01 g accelerometer. The orientation of the low-range accelerometers is shown in figure 5. Vehicle attitude and spin rate were sensed by three mutually perpendicular magnetic aspect sensors and four sun sensors, respectively. Rocket sustainer chamber pressure, oxidant tank pressure, and fuel-tank pressure were monitored throughout the flight. The turntable rate-gyro signal and other performance parameters were also measured.

Experiment performance instrumentation. - The locations of the temperature transducers on the hydrogen sphere are given in figure 6. Hydrogen-tank pressure was measured throughout the flight by two pressure transducers, one for 0 to 50 and one for 0 to 200 pounds per square inch absolute. The liquid-hydrogen level was determined visually prior to launch from a scale mounted on the inside surface of the hydrogen tank (fig. 2). Hydrogen boiloff during prelaunch operations and up to vehicle lift-off was measured by a laboratory displacement-type gasmeter. Motion pictures of the interior of the hydrogen tank during the experimental portion of the trajectory were obtained by a 35-millimeter motion-picture camera having an optical system that provided a field of view somewhat greater than 90°. This camera was started simultaneously with the power for the heater sphere and operated in conjunction with a high-intensity strobe light. The film rate was 5 frames per second, and each frame provided a pulse on the telemeter record for synchronization of the photographs with other telemetered information. A 1-inch-diameter glass sphere, 40 percent filled with alcohol having a dye additive, was positioned in the nose cone and illuminated in such a way that a side view of it would appear next to the hydrogen sphere in each picture. The purpose of this smaller sphere was to make pos-

sible a visual determination of any vehicle motions that might affect the results of the experiment. The rocket nose cone containing the camera was separated from the rocket and payload at the end of the experiment, parachuted back to Earth, and recovered.

PROCEDURE

Because of the vacuum between the hydrogen tank and the outer sphere, it was necessary to cool the experiment for several hours prior to installation on the launch vehicle to enable the heater shell to attain liquid-nitrogen temperature. This was done by flowing liquid nitrogen continuously through the cooling coils on the outer sphere and keeping the inner hydrogen tank filled with liquid hydrogen. About $2\frac{1}{2}$ hours prior to scheduled lift-off, the hydrogen tank level was set approximately at the level desired for flight, and the hydrogen tank, the instrument tower, and the nose cone were installed on the rocket. Just prior to installation of the nose cone, the liquid-hydrogen level was visually measured for the last time and recorded. The hydrogen boiloff rate was metered from that time until rocket lift-off and was used to determine the actual hydrogen level at lift-off. Liquid nitrogen was kept flowing in the outer-sphere coils until rocket lift-off to keep the hydrogen boiloff rate at a minimum.

At rocket booster ignition, the hydrogen vent valve was automatically closed, and an onboard sequence timer was started. Figure 7 gives a plot of vehicle altitude against time and is marked with the major events of the flight. At 39 seconds after lift-off the camera was turned on along with heater-sphere power, and from that time until separation of the nose cone pictures were taken of the interior of the hydrogen tank. Rocket sustainer burnout occurred 53 seconds after lift-off, and drag-cancellation operated from then until 72 seconds. The despin operation was started at 72 seconds and was complete by 118 seconds. The true weightless period of the flight lasted from that time until 294 seconds, when a small thrust was produced to collect and mix the fluid by using fuel tank gas. The nose cone was separated from the rocket vehicle and payload at 331 seconds and was subsequently recovered.

RESULTS AND DISCUSSION

The flight described was conducted at Wallops Island, Virginia. The experiment consisted of a 9-inch-diameter spherical tank, nonuniformly heated, containing 25.1 percent liquid hydrogen by volume at rocket lift-off. The results given herein are based on telemetered data received at Wallops Island from the rocket.

Rocket Performance

The rocket-vehicle-casing roll-rate history is shown in figure 8. The value of rocket roll rate at sustainer burnout was somewhat higher than predicted, and thus the total despin time was about 45 seconds instead of the predicted 25 sec-

onds. This did not affect the results of the experiment, except to shorten the weightless period. The payload or nonspinning portion of the vehicle moved through a total angle of about 30° from lift-off through the end of the flight.

The accelerations seen by the rocket and payload are shown in figures 9 and 10. Figure 9 gives the longitudinal acceleration history. The full-scale range of the accelerometer was $\pm 10^{-2}$ g. The drag-cancellation thrust caused an off-scale positive signal until about 65 seconds, and this positive acceleration slowly decayed until 72 seconds when the antidrag thrust was ended. The acceleration immediately became negative, because the vehicle was still encountering a small drag force, but then slowly returned to zero as the drag diminished. The acceleration was less than 5×10^{-4} g until about 190 seconds, when a small positive acceleration of about 10^{-3} g was produced. A backup accelerometer on the rocket confirmed that this acceleration actually existed and was not a malfunction in the measuring instrument. From observations of the fuel-tank pressure history, it was determined that the probable cause of this small acceleration was a leaking valve that allowed some of the gas to escape. At 294 seconds, the collection thrust was applied by utilizing residual fuel-tank pressure, and a peak acceleration of about 12×10^{-3} g resulted. At about 340 seconds the accelerations became off-scale negative, which indicated that the vehicle was beginning to tumble as it reentered the atmosphere and exerted a centrifugal force on the accelerometers. Figure 10 gives the accelerations along mutually perpendicular lateral axes. Prior to about 100 seconds, both accelerometers oscillated between positive and negative values, the peak being roughly $\pm 25 \times 10^{-3}$ g. These oscillations were similar to those described in reference 5 and were caused by a small misalinement between the spin axes of the stationary payload and the spinning rocket casing. The amplitude of the oscillation diminished to zero as the rocket casing was despun. Thereafter the accelerations were near zero until the vehicle reentered the atmosphere, when they began slowly to alternate between positive and negative as aerodynamic forces induced vehicle tumbling.

Experiment Performance

Liquid-hydrogen level. - The liquid hydrogen used for this experiment was 97 percent para-hydrogen. The liquid-hydrogen level at lift-off was calculated from the curve of figure 11 and the last visual reading. The liquid-hydrogen level at launch was 25.1 percent by volume. This corresponds to a liquid-hydrogen weight of 0.2453 pound and a hydrogen-vapor weight of 0.01384 pound. The vapor fraction at lift-off was 5.34 percent, and the system density was 1.173 pounds per cubic foot. The system density was a constant for the flight and is defined as the total hydrogen weight (liquid plus vapor) divided by the container volume.

Fluid motion and configuration. - The motion of the fluid throughout the the flight can be best explained by reference to the plots of the inner-sphere skin temperature and the pictures obtained from the 35-millimeter films. Figure 12 presents a plot of the temperature histories of sphere transducers 4 and 16, one located on the upper side of the sphere close to the rocket spin axis and the other similarly positioned on the lower half. The temperature histories

of the remaining sphere transducers are shown in figure 13. Prior to launch, and during the burning period, the fluid remained in the lower portion of the sphere, as evidenced by the fact that transducer 4 read the saturation temperature, while transducer 16 was much warmer. Figure 14(a) shows a picture of the sphere taken prior to burnout. The fluid surface was covered with ripples generated by vibration from the rocket combustion process. The white spot in the center of the picture was most likely an agglomeration of frozen impurities in the hydrogen. These impurities had been observed in previous flights. At 53 seconds the sustainer burned out, and the inner-sphere wall became entirely wetted shortly thereafter. Transducer 16 indicated a sharp drop in temperature as that portion of the wall became wetted (fig. 12(b)). Figure 14(b) shows two pictures, one taken just before and the other immediately after the drop in temperature. The blurred quality of the picture as the lens became covered with liquid is evident. A sequence of pictures taken during the drag-cancellation operation (fig. 14(c)) indicates that the fluid was swirling in a counter-clockwise direction. This swirling motion most likely arose from the small rotating lateral acceleration produced by the aforementioned misalinement between the payload and the rocket. The despin operation was initiated at 73 seconds. The counter-clockwise motion of the fluid apparently diminished, and throughout most of this operation the fluid moved in a random fashion. A typical despin picture (fig. 14(d)) displays many of what were probably light-source images produced by the moving hydrogen. Despin was complete at 118 seconds, but the films indicate that the fluid still had some residual motion. Pictures taken after despin (fig. 14(e)) disclose some small, irregularly shaped objects moving in the fluid that were either particles from the agglomeration of impurities mentioned previously or specular reflections of the light from liquid surfaces. In either case, there was residual fluid motion, since these objects moved about. The fluid was relatively quiet by about 165 seconds. Some residual motion of the fluid that was slow to damp out might have been present because of the very low viscosity of the fluid.

At 230 seconds, transducer 16 showed a sharp increase in wall temperature, which indicated that vapor was again next to this portion of the wall. Reference to figure 13 shows that this drying off of the upper part of the sphere started near the fill and vent tube at 180 seconds since transducer 18 was the first to dry off. This drying-off phenomenon had been observed in each of the three previous Aerobee flights. The two most likely causes of this phenomenon are

(1) The top of the sphere was covered by a very thin layer of liquid that completely vaporized.

(2) Liquid was drawn by capillary action into the vent line, was vaporized by the warmer temperature, and was reemitted as a vapor; thus, a vapor pocket was formed. Calculations made of the heat conducted through the fill tube do not indicate an abnormally large heat leak at this point. In any case, the vapor pocket continued to grow, as indicated by transducers 11, 15, and 19, and, as might be expected, the rate of growth was faster toward the warm portion of the hydrogen sphere. This can be seen from the fact that transducer 11 warmed up sooner and faster than transducer 19, which was closer to the fill tube and at a greater latitude but on the cool side of the sphere.

In addition, the films indicate some small round objects in the fluid at about 165 seconds (fig. 14(f)). It is felt that they were not the light-source images present during despin because they lacked the diffuse quality of these, and they were probably not impurity particles, since they were round. Hence, they were probably vapor bubbles formed by the radiant heating. They were apparent only in the area near the light source, and they appeared to be in motion in a general direction toward the light source and the upper part of the sphere. The number and size of the bubbles increased as time progressed, particularly from about 260 seconds on (fig. 14(g)). These bubbles are discussed in more detail in the section "Heat-transfer mechanism."

At 294 seconds the 12×10^{-3} g collection acceleration was applied. Transducer 16 dropped somewhat in temperature, and it is believed this was due to the sloshing initiated by this operation. Figure 14(h), a sequence of pictures taken shortly after collection, shows that the fluid oscillated, first formed a ball in the center of the sphere and then spread out around the edge. The liquid was not driven completely down the walls by this disturbance, however, as evidenced by the fact that wet transducers near the edge of the drying-off area remained wet after collection. The oscillation continued, with slowly decreasing amplitude, until nose-cone separation.

The 1-inch-diameter glass sphere containing alcohol, described previously, appears in each picture of the hydrogen sphere. The behavior of the alcohol in the present experiment followed the general pattern set forth in reference 7.

Heat-Transfer Characteristics

Heat transferred to hydrogen. - Figure 15 presents the temperature histories of the heater segments. The desired control temperatures for each of the two heater segments that encompassed a 45° arc was 405° R, and that for the 90° segment was 455° R. The remaining hemisphere was fastened to the outer-sphere wall by stainless-steel legs and was not electrically heated; this segment assumed a temperature slightly above that of liquid nitrogen. This temperature remained nearly constant throughout the flight, as shown in figure 15(d). The difference in the readings of the two transducers is believed to have been due to a combination of the facts that the upper and lower parts of the segment were fabricated separately and that some temperature gradients were established in the outer structural sphere by the liquid-nitrogen flow. The temperature of this segment was taken as the average of the two readings.

The time history of the rate of heat absorption by the hydrogen mass throughout the flight is shown in figure 16. The method used to calculate the values shown in this plot is described in appendix A. The total heat-absorption rate increased steadily from 40 seconds after lift-off as the heater temperatures climbed. The absorption rate reached a peak shortly after burnout because the liquid was completely wetting the walls and was absorbing heat from the wall portions that had been relatively hot. The absorption rate dropped as the walls became cool, but rose again to a local maximum at about 80 seconds as the heaters approached their control temperatures. Thereafter, the absorption rate held nearly constant and dropped slowly because of the slight drop in heater

temperatures. There was a localized decrease at around 240 to 280 seconds as the upper wall of the tank dried off and warmed up, as described previously. This warming up caused the tank wall to contain more heat and left less available for absorption by the hydrogen. The integration of the curve in figure 16 to obtain the total heat input was arbitrarily started at 40 seconds and is presented in figure 17. A total of 2.9 Btu was absorbed by the hydrogen by the time of collection.

Hydrogen pressure. - The hydrogen pressure history observed in flight is shown by the symbols in figure 18. Also plotted in figure 18 (as a solid curve) is the pressure history that would have resulted if all the heat absorbed by the hydrogen had contributed to raising the bulk temperature of the fluid (i.e., uniform fluid temperature throughout). This pressure history was calculated as described in appendix A. The hydrogen pressure rise from lift-off, when the vent valve was closed, until 40 seconds, when the heaters were turned on, was less than the accuracy of the measuring instrumentation since the heat input was solely from conduction and radiation heat leaks. Shortly after the heaters went on, the pressure began to rise faster; the rate of increase reached its maximum at approximately 100 seconds, and thereafter the pressure increased steadily with time until the end of the flight. It can be observed from figure 18 that the measured pressure rose faster than the homogeneous pressure. This is a phenomenon that has been observed in all Aerobee liquid-hydrogen experiments to date (refs. 5 to 7). The fact that figure 18 shows that the measured pressure was greater than the homogeneous pressure after 170 seconds indicates that the liquid-vapor interface that dictates system pressure was at a greater temperature than that for a uniform fluid temperature. Therefore, to satisfy thermodynamic considerations, it must be assumed that a portion of the fluid in the hydrogen tank was at a temperature lower than that of equilibrium. A similar result was obtained in previous Aerobee flights in which the heating was uniform (refs. 5 and 6). The conclusion was reached in these reports that the general form of the gradient is one in which the fluid temperature is near the saturation temperature at the wall, decreases to a minimum somewhere between the wall and interface, and increases again to the saturation temperature at the liquid-vapor interface. Figure 19 shows that, in the present experiment, the cool side of the tank wall was within 0.5° R of the saturation temperature throughout the flight, whereas the warm side remained approximately 1° R higher. Furthermore, no noticeable decrease in hydrogen pressure at the time of collection could be detected (fig. 18), despite the fact that the motion pictures show considerable fluid mixing at this time. This would indicate either that the relatively small collection thrust obtained was not sufficient to thoroughly mix the fluid and destroy the temperature gradient established during weightlessness, or that the magnitude of this gradient was smaller than that indicated by the hydrogen pressure rise. It is also possible that the collection operation left only a thin layer of liquid on the upper tank wall, which tended to boil away rapidly and masked any pressure decrease.

Heat-transfer mechanism. - It is apparent from the foregoing results that heat was carried away from the tank wall and distributed within the hydrogen in some manner such that the hydrogen vapor temperature rose above the average liquid temperature. The mechanism by which this could have been accomplished in the case of uniform heating is discussed at length in reference 5, where the

conclusion is reached that the only process that would satisfactorily explain the observed results is nucleate boiling of the liquid. A similar conclusion is reached in references 6 and 7. In the present experiment, pictures of the hydrogen-tank interior were obtained that show the formation and movement of vapor bubbles and support the nucleate-boiling theory.

As shown in figure 14, objects that were most likely bubbles appeared at about 165 seconds after lift-off. At that time, the size of the bubbles was small and there were relatively few of them. The apparent motion was generally upward and toward the light source, with perhaps a slight counterclockwise swirling. It is possible that some fluid motion from despin still existed at that time. Some bubbles rose to a certain point and then moved back toward the bottom of the tank (fig. 20(a)). The change in direction may have been only an optical effect, however. At about 243 seconds, the number of bubbles diminished, and the rate of bubble motion became very small, which indicated the damping out of residual fluid motion. From that time on, the bubble population and rate of movement increased quickly. Figure 20(b) shows a series of pictures taken at about 280 seconds. The liquid surface seen by the camera was disturbed by many small ripples (the sphere temperatures indicated that liquid was no longer covering the lens). The bubbles were again moving rapidly upward past the light source, and many of them were quite large. A number of points appeared on the liquid surface from which ripples spread out in every direction; these points were probably the sites of vapor bubbles that broke the surface and joined the large ullage bubble.

The foregoing remarks are based on observations of the bubbles in the vicinity of the light source, because they were most easily seen in that location. It is believed, however, that, because of the much larger radiant heating rate on the side of the tank away from the light source, the majority of the bubbles were formed on that side of the tank. There they were not easily detected, however, since they were not illuminated from behind and were masked by shadows cast by the bubbles near the light source.

While bubble motion in the earlier portion of the weightless period was most likely due to residual fluid motion induced after burnout, it is not felt that the bubble motion in the later part of the flight can be attributed entirely to this cause, since an apparently quiescent period was reached in the liquid at about 240 seconds. Furthermore, since the bubbles were not distorted, it can be assumed that they were moving with the fluid, rather than through it. Further evidence to support the possibility of fluid circulation is furnished by figure 19, wherein the average liquid-wetted-wall temperatures are compared with the saturation temperature corresponding to the existing pressure. The average sphere temperature was the same for both the warm and the cool sides of the tank prior to heater starting. Shortly after the heaters began to warm up, however, an average temperature difference of about 1.5° R was established between the warm and the cool sides, and this difference held fairly constant throughout the remainder of the flight. Because of the averaging process, it is believed that this temperature difference is representative of the actual flight value, despite the fact that the individual sphere temperatures can be assumed accurate only to $\pm 1^{\circ}$ R. A much greater temperature difference than 1.5° R would be required to support the heating rate necessary to warm the cool side of the

tank at the indicated rate if conduction were the only heat-transfer mechanism assumed. It is probable that the rate of temperature rise of the cool side followed that of the warm side closely in spite of the wide disparity in heating rates because fluid circulation caused a distribution of the absorbed heat within the hydrogen.

The net result of the preceding observations is to indicate that fluid motion, or circulation, occurred during the last 40 to 50 seconds of weightlessness. This fluid motion was not due to convection currents, as the accelerations during that period were less than 5×10^{-4} g. It was also not due to residual fluid motion from postburnout disturbances, because a quiescent period occurred in the fluid at 240 seconds. It is possible that this fluid motion was induced by bubbles forming on the tank wall and thereby imparting some momentum to a portion of the liquid. This momentum would have been dissipated very slowly because of the low viscosity of the liquid. As the bubble population and the resulting fluid motion increased, the bubbles would have been picked from the wall and carried about by the circulating fluid. It is possible that the circulation arose from the nonuniform nature of the radiant heating. It should be noted in this connection that, in previous Aerobee flights, in which the heating was uniform, sufficient photographic evidence was not obtained to enable any conclusions to be drawn regarding circulation of the fluid.

CONCLUDING REMARKS

An experiment to determine the behavior of the partially filled liquid-hydrogen tank under simultaneous conditions of weightlessness and nonuniform radiant heat addition was flown on an Aerobee 150A sounding rocket. The flight was normal, with no severe tumbling maneuvers, and a weightless time of approximately $3\frac{1}{2}$ minutes was provided. The trajectory apogee was 94 statute miles with a payload of 277 pounds. The radiant heating of the tank was nonuniform; the maximum heating rate was 61.5 Btu per hour per square foot on the warm side and approximately 1 Btu per hour per square foot on the cool side.

Shortly after burnout, the entire interior surface of the hydrogen tank became liquid wetted, which indicated that the large ullage vapor bubble was at or near the center of the tank. Approximately midway through the flight the upper portion of the tank began to dry off, and this process continued until the end of the flight, at a faster rate toward the warm side of the tank and more slowly toward the cool side. This phenomenon had occurred in all prior Aerobee liquid-hydrogen experiments.

The measured hydrogen pressure during the flight was larger than the pressure calculated by assuming thermal equilibrium during the last half of the flight, and the difference between the two increased as time progressed. This result is also similar to results observed in all previous Aerobee flights.

The photographs support the nucleate-boiling theory of heat transfer within the fluid put forth in previous reports and also indicate the probability of circulation within the fluid during weightlessness.

Lewis Research Center
National Aeronautics and Space Administration
Cleveland, Ohio, September 13, 1963

CONFIDENTIAL

APPENDIX A

DETERMINATION OF HEAT ABSORPTION BY HYDROGEN DURING FLIGHT

It is possible to derive an expression for the heat transferred between concentric spheres when each sphere is at a uniform temperature (ref. 8). This method is outlined and used in references 5 to 7 to calculate the heat absorbed by the hydrogen mass during flight.

For the present experiment, however, the heater configuration was such that the heating rate was nonuniform. Because of the different temperatures associated with the various heater segments and the associated effects such as heater-shell end effects and heat transfer directly between heater segments, which are not present with uniform heating, it was expected that the value calculated by applying the concentric-sphere theory to each heater segment would be different from the actual heat absorbed by the hydrogen. To confirm this, a ground test was conducted.

A hydrogen Dewar identical to that used in the flight was filled with liquid hydrogen to approximately the same level. The vent valve was closed, and the heaters were turned on and allowed to control the heater segment temperatures as in flight. The heaters were kept on for a length of time equal to the duration of the flight. During this test the sphere was continually shaken so as to mix the fluid and destroy any temperature gradients that might form in the liquid. The hydrogen pressures and the heater temperatures were recorded. From the pressure rise and the fact that the hydrogen in the Dewar was at all times in thermal equilibrium because of continuous mixing, it was possible to obtain the heat absorbed by the hydrogen as a function of time by using the known thermodynamic properties of hydrogen.

Heat-Transfer Equations

The amount of heat absorbed by the hydrogen is equal to the heat transferred to the sphere by radiation, solid conduction, and gaseous conduction less the amount of heat stored in the container itself. This heat is given by

$$\Delta Q_{abs} = (\dot{Q}_r + \dot{Q}_{sc} + \dot{Q}_{gc})\Delta t - \Delta Q_s \tag{A1}$$

(Symbols are defined in appendix B.)

The heat transferred by thermal radiation between two concentric spheres is given by reference 5 as

$$\frac{\dot{Q}_r}{A_s} = \frac{\sigma(T_h^4 - T_s^4)}{\frac{1}{\epsilon_s} + \frac{A_s}{A_h}\left(\frac{1}{\epsilon_h} - 1\right)} \tag{A2}$$

In the calculation of the radiant heat transfer for the unsymmetrical heater configuration, equation (A2) was applied to each heater segment separately in conjunction with that portion of the hydrogen tank in a radial line with it. The calculation was insensitive to T_s for this configuration because of the relatively high value of T_h.

The heat transferred by solid conduction is given by

$$\frac{\dot{Q}_{sc}}{A_{sc}} = \frac{k}{l} \Delta T \tag{A3}$$

The heat transferred by gaseous conduction is given in reference 5 as

$$\frac{\dot{Q}_{gc}}{A_s} = K \frac{\gamma + 1}{\gamma - 1} \frac{\alpha_s \alpha_h}{\alpha_h + \alpha_s (1 - \alpha_h) \frac{A_s}{A_h}} \frac{P_G}{\sqrt{MT_G}} (T_h - T_s) \tag{A4}$$

where K is a numerical constant that depends on the units used. Reference 5 also indicates that, for heating rates of 160 Btu per hour per square foot, the effect of gaseous conduction on the heat transfer is negligible for vacuums less than 0.03 micron of mercury. Upon extrapolating this result to the present heating rate (average, approx. 25 Btu/(hr)(sq ft)) and vacuum (less than 0.002 micron Hg throughout the flight), the gaseous conduction was found to be negligible for the present experiment.

The heat absorbed by the container wall is given by

$$\Delta Q_s = W c_p \Delta T_s \tag{A5}$$

Heat Transferred in Ground Test

The rate of heat transfer from each heater segment was calculated for the ground test by using equation (A2) with the pertinent heater temperature. The radiative and conductive heat leak rate and the rate of heat absorption in the container itself were calculated by using equations (A3) and (A5). These calculations were identical in form to those described in reference 5.

Next, the actual heat absorbed by the hydrogen during the ground test was obtained from the measured pressure rise, the known thermodynamic properties of hydrogen as presented in reference 9, and the fact that for a closed, constant volume system

$$\Delta Q = \Delta U \tag{A6}$$

From the heat-absorption history thus obtained was subtracted the calculated integrated heat-leak history. The remainder was assumed to represent the portion of the actual heat absorbed that was radiated by the heater segments alone.

Finally, the ratio of measured heat absorption to that calculated from equation (A2) was determined. The average value of this ratio was assumed to represent a combination emissivity and configuration factor resulting from the nonuniform nature of the heating. Figure 21 presents histories of the measured and calculated heat inputs to the liquid hydrogen during the ground test.

Heat Transferred During Flight

A calculation identical to that made for the ground test was made of the rate of heat produced by the heater segments by using the flight heater temperatures and other pertinent data. This heater segments radiation history was multiplied by the emissivity configuration factor determined by the ground test. The result then represented the actual rate of heat produced by the flight-heater segments. The heat-leak and container-absorption rates were calculated by using the flight data and added to the heat produced by the heater segments. The sum, representing the history of the total rate of heat absorption by the liquid hydrogen during flight, is shown in figure 16.

APPENDIX B

SYMBOLS

A	area, sq ft
c_p	specific heat, Btu/(lb)($^\circ$R)
H	enthalpy, Btu/lb
k	thermal conductivity, (Btu)(in.)/(hr)(sq ft)($^\circ$R)
l	length of conduction path, in.
M	molecular weight
P	pressure, lb/sq in. abs
P_G	gage pressure, microns Hg
Q	heat, Btu
$\dot{Q}$	heat-transfer rate, Btu/hr
$\dot{Q}_{gc}$	heat transferred to hydrogen sphere by gaseous conduction, Btu/hr
$\dot{Q}_r$	heat transferred to hydrogen sphere by radiation from heater, Btu/hr
$\dot{Q}_{sc}$	heat transferred to hydrogen sphere by solid conduction, Btu/hr
T	temperature, $^\circ$R
T_G	temperature of gage that measures P_G, $^\circ$R
U	internal energy, Btu/lb
v	specific volume, cu ft/lb
W	weight of hydrogen tank, lb
α	accommodation coefficient
γ	ratio of specific heats
ϵ	total hemispherical emissivity
σ	Stefan-Boltzmann constant, 0.1713×10^{-8} Btu/(hr)(sq ft)($^\circ$R)^4

CONFIDENTIAL

Subscripts:

abs	absorbed
gc	gaseous conduction
h	heater
s	hydrogen tank wall
sc	solid conduction

REFERENCES

1. Reynolds, William C.: Hydrodynamic Considerations for the Design of Systems for Very Low Gravity Environments. Rep. LG-1, Stanford Univ., Sept. 1, 1961.

2. Benedikt, E. T.: General Behavior of a Liquid in a Zero or Near Zero Gravity Environment. Rep. ASG-TM-60-9Z6, Noraic Div., Northrop Corp., May 1960.

3. Petrash, Donald A., Nelson, Thomas M., and Otto, Edward W.: Effect of Surface Energy on the Liquid-Vapor Interface Configuration During Weightlessness. NASA TN D-1582, 1963.

4. Papell, S. Stephen: An Instability Effect on Two-Phase Heat Transfer for Subcooled Water Flowing Under Conditions of Zero Gravity. Paper 2548-62, Am. Rocket Soc., Inc., 1962.

5. Knoll, Richard H., Smolak, George R., and Nunamaker, Robert R.: Weightlessness Experiments with Liquid Hydrogen in Aerobee Sounding Rockets; Uniform Radiant Heat Addition - Flight 1. NASA TM X-484, 1962.

6. McArdle, Jack G., Dillon, Richard C., and Altmos, Donald A.: Weightlessness Experiments with Liquid Hydrogen in Aerobee Sounding Rockets; Uniform Radiant Heat Addition - Flight 2. NASA TM X-718, 1962.

7. Nunamaker, Robert R., Corpas, Elias, L., and McArdle, Jack G.: Weightlessness Experiments with Liquid Hydrogen in Aerobee Sounding Rockets; Uniform Radiant Heat Addition - Flight 3. NASA TM X-872, 1963.

8. Brown, Aubrey I., and Marco, Salvatore M.: Introduction to Heat Transfer. Second ed., McGraw-Hill Co., Inc., 1951.

9. Roder, Hans M., and Goodwin, Robert D.: Extended Tables of Provisional Thermodynamic Functions for Para Hydrogen (British Units), in Liquid, Fluid and Gaseous States at Pressures to 5000 PSI., 36 to 180° R and at Pressures to 1500 PSIA., 140 to 540° R. Rep. 7220, Nat. Bur. Standards, Jan. 3, 1962.

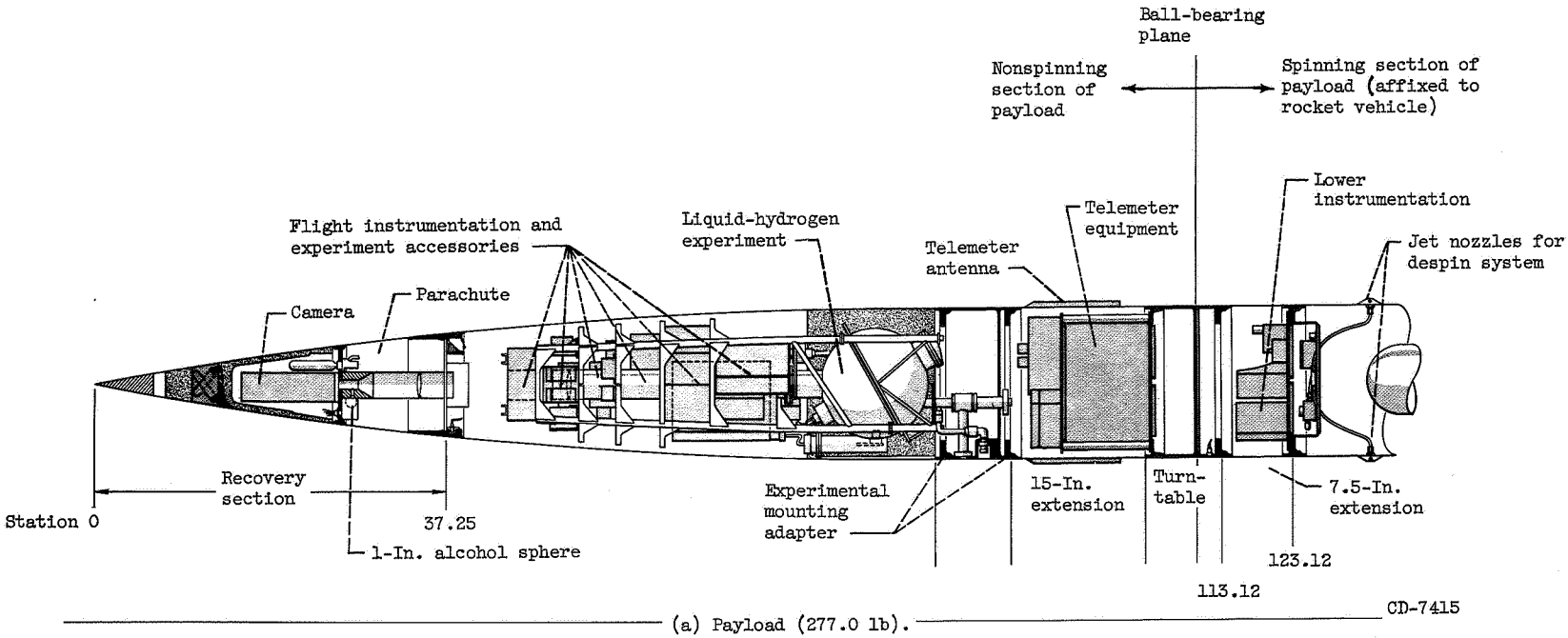

(a) Payload (277.0 lb).

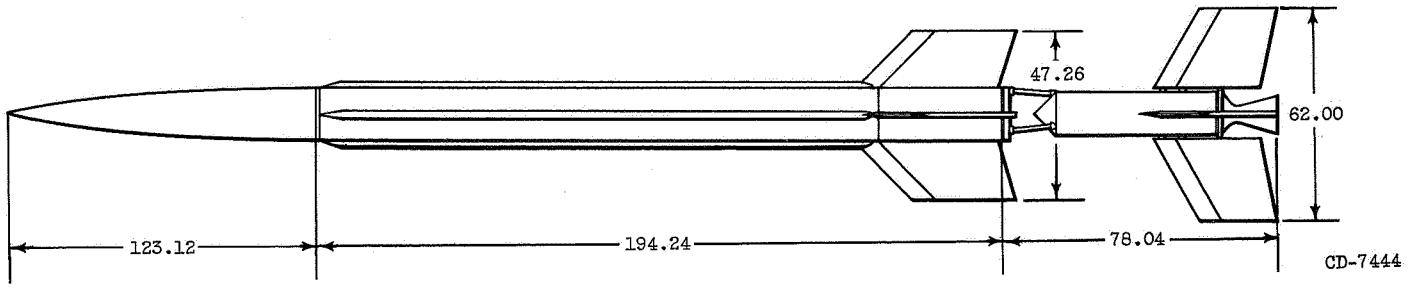

(b) Aerobee 150A rocket.

Figure 1. - Rocket vehicle and payload. (Dimensions in inches.)

CONFIDENTIAL

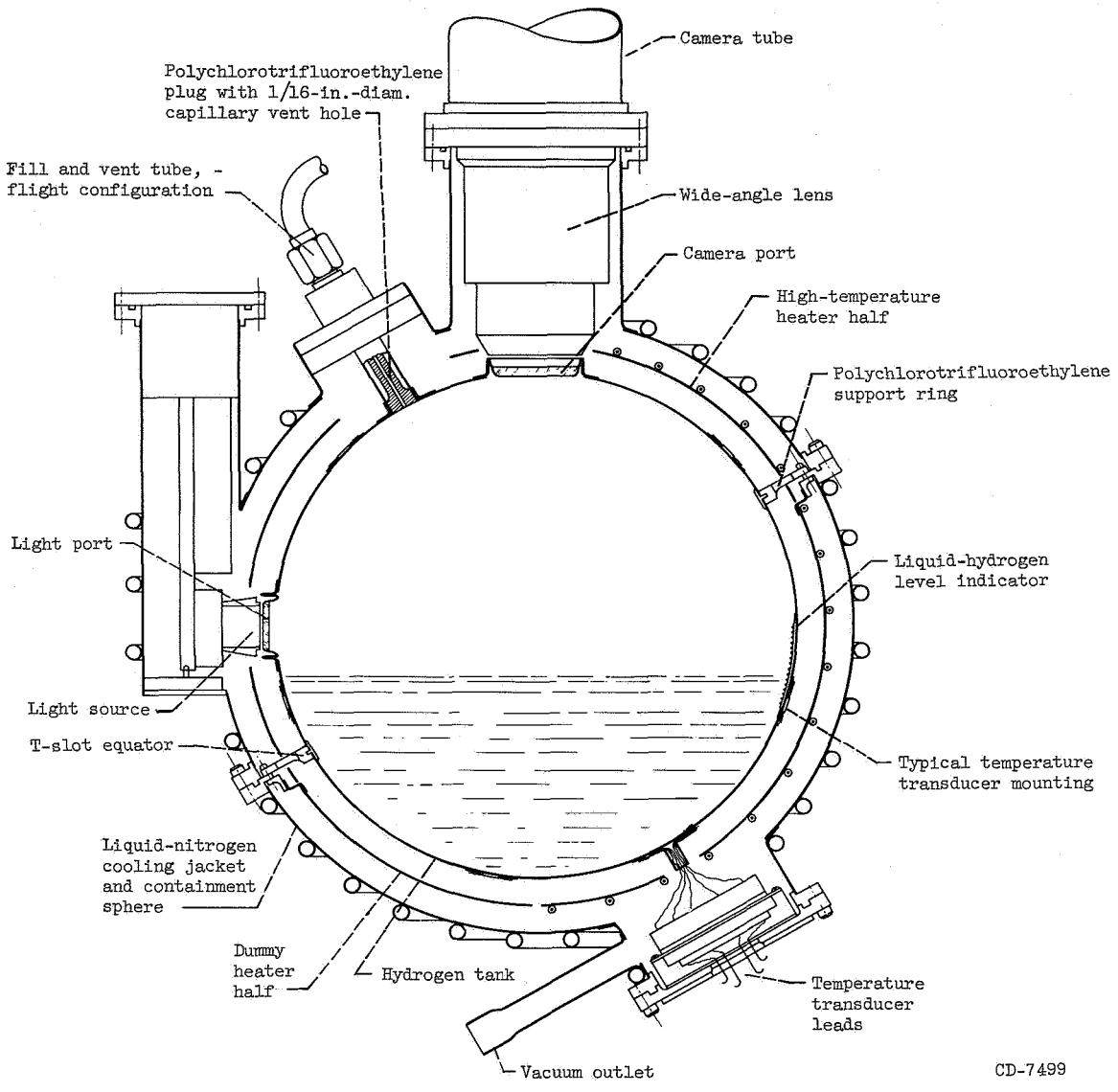

Figure 2. - Cross section of zero-gravity heat-transfer experiment.

DECLASSIFIED

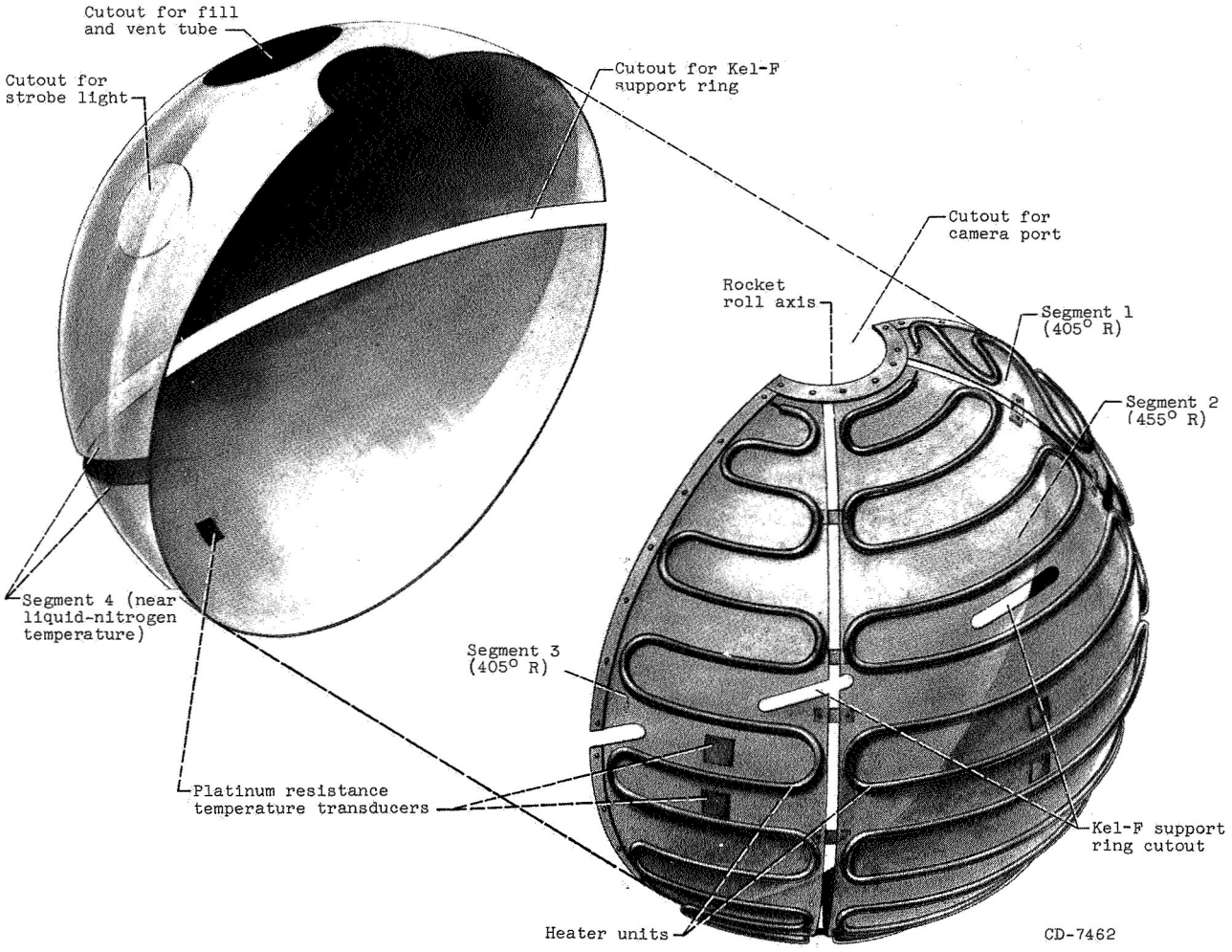

Figure 3. - Drawing showing details of segmented unsymmetrical heater arrangement. All interior surfaces painted flat black.

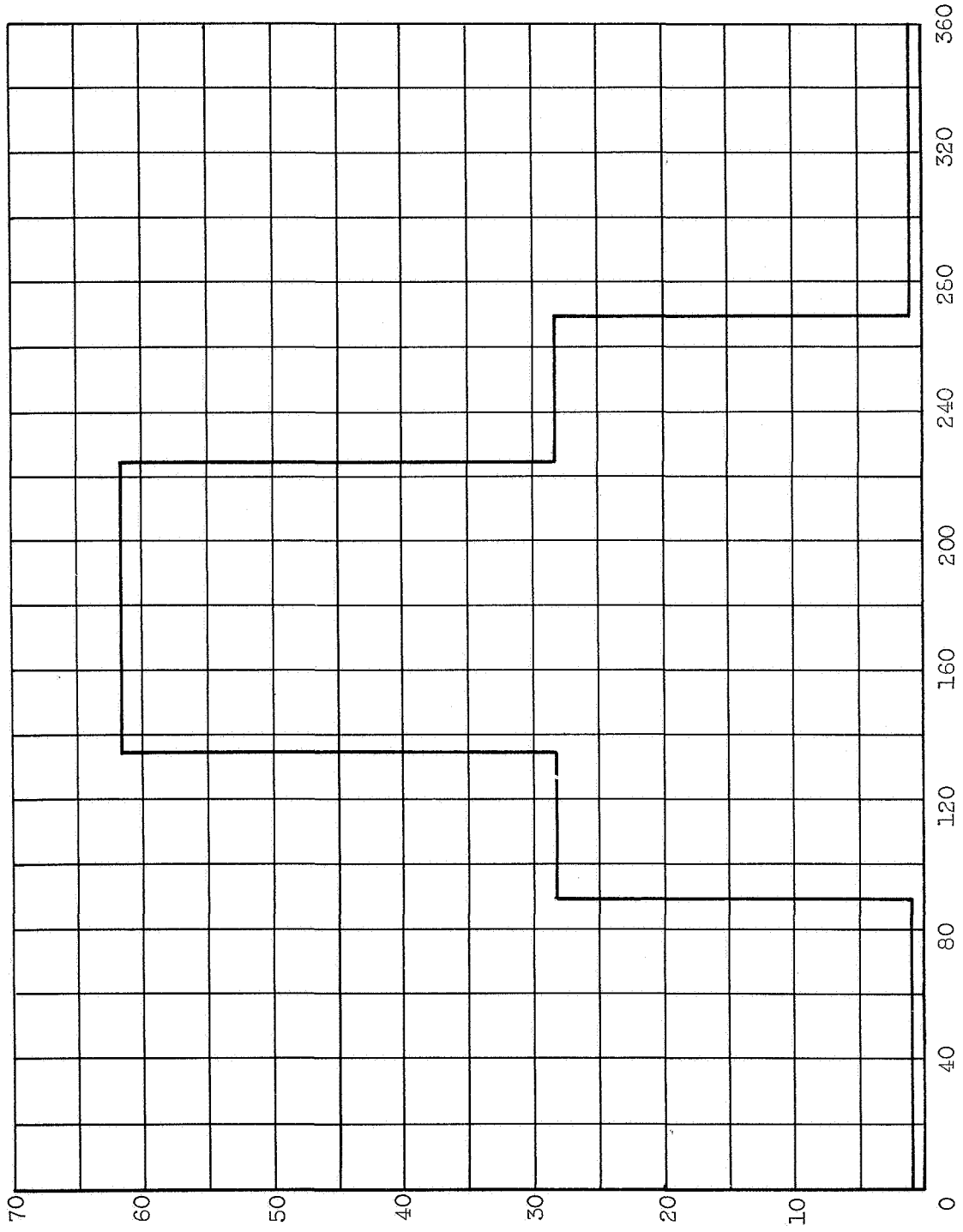

Figure 4. - Nominal heat-transfer rate to liquid hydrogen as function of longitude on hydrogen tank.

CONFIDENTIAL

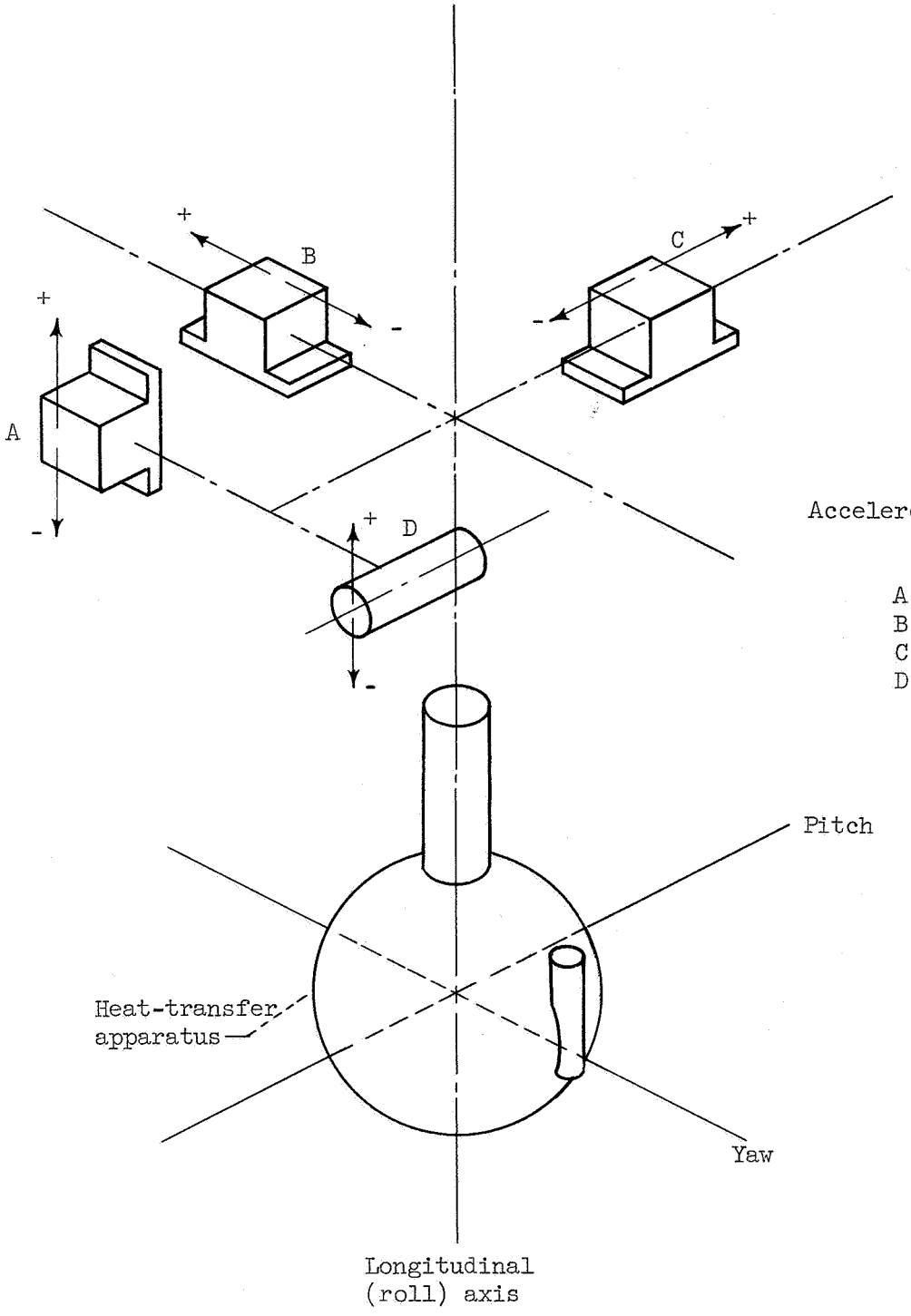

Accelerometer	Full-scale range, g's
A	$\pm 10^{-2}$
B	$\pm 10^{-2}$
C	$\pm 10^{-2}$
D	$\pm 10^{-3}$

Figure 5. - Low-range-accelerometer orientation.

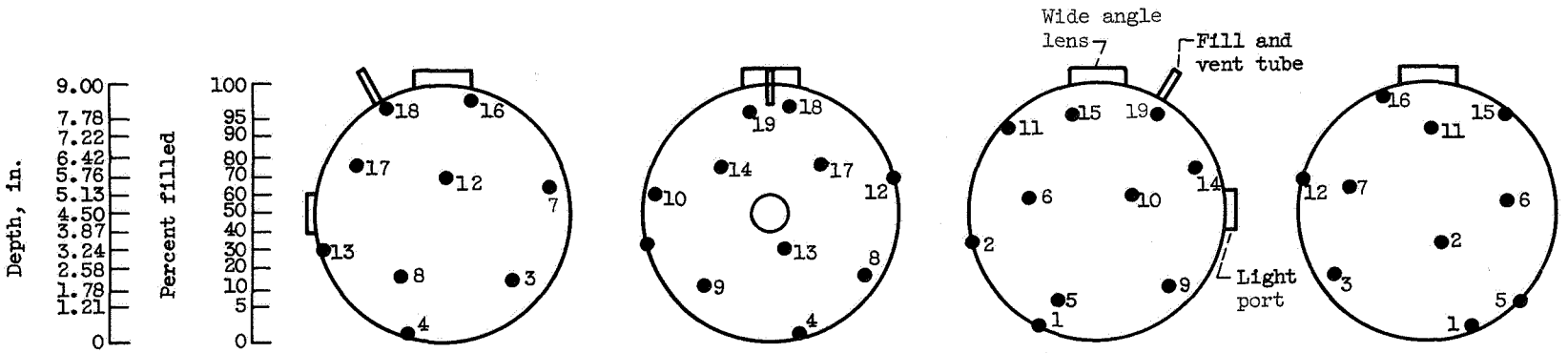

(a) Temperature transducer general location. Spheres progressively rotated 90°.

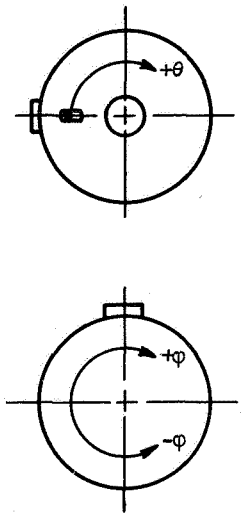

Temperature transducer	φ, deg	θ, deg	Temperature transducer	φ, deg	θ, deg
1	-60	154	11	44	172
2	-15	172	12	18	273
3	-32	240	13	-16	354
4	-73	330	14	19	28
5	-43	111	15	57	94
6	5	129	16	67	257
7	13	218	17	24	328
8	-28	298	18	64	340
9	-37	46	19	54	28
10	5	78			

(b) Spherical coordinate location.

Figure 6. - Location of temperature transducers on inner sphere of experiment.

CONFIDENTIAL

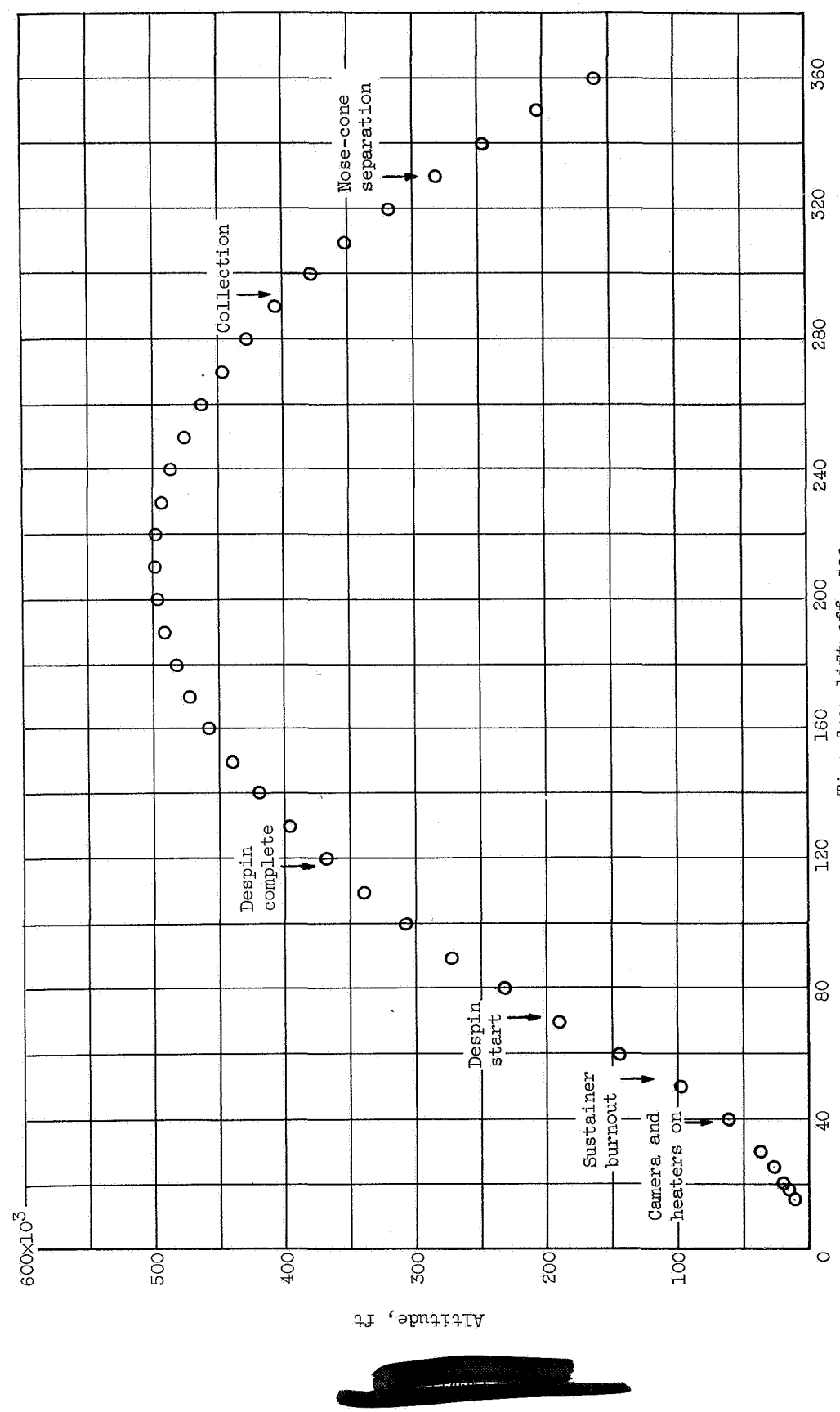

Figure 7. - Vehicle trajectory.

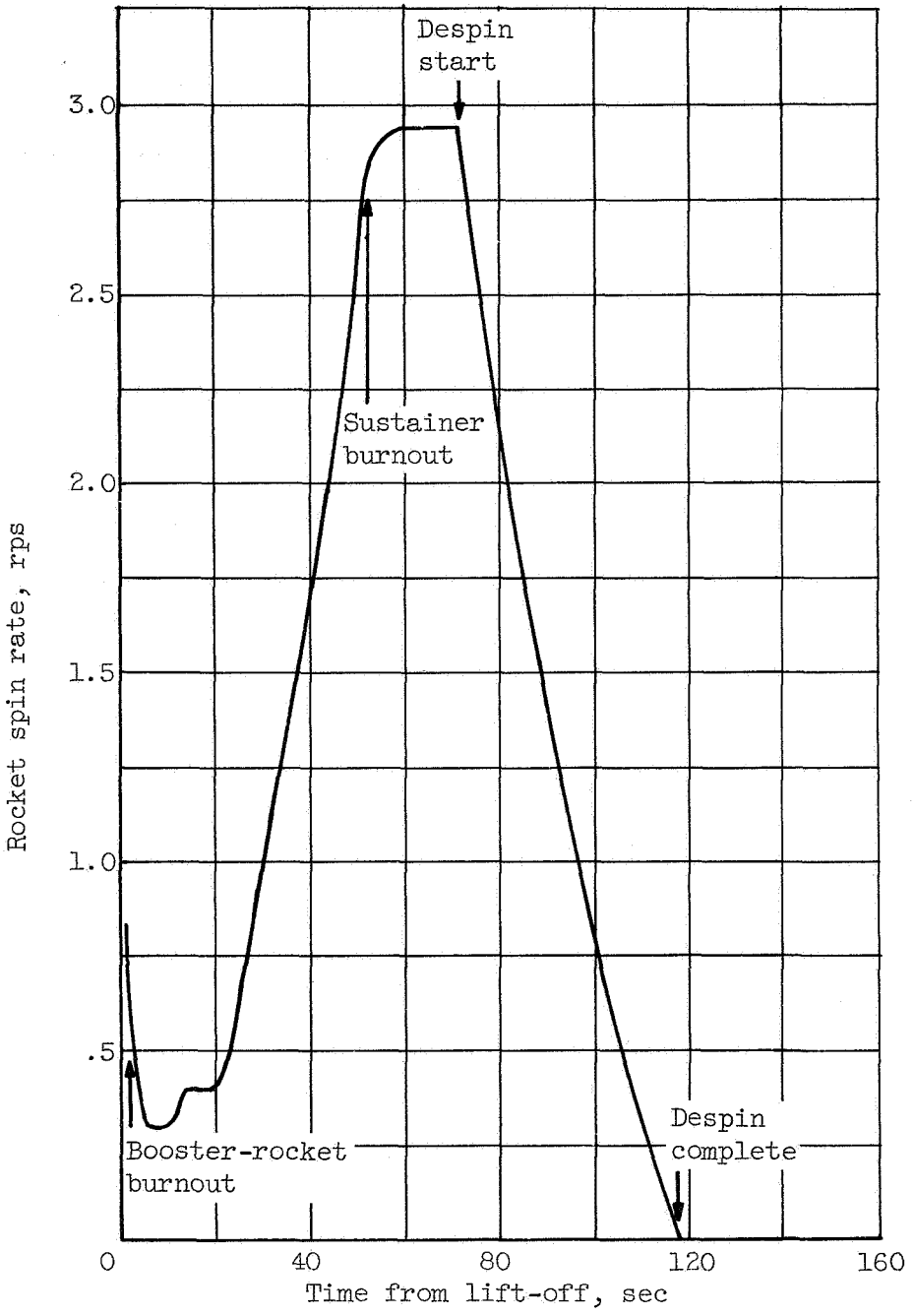

Figure 8. - Rocket-vehicle roll-rate history.

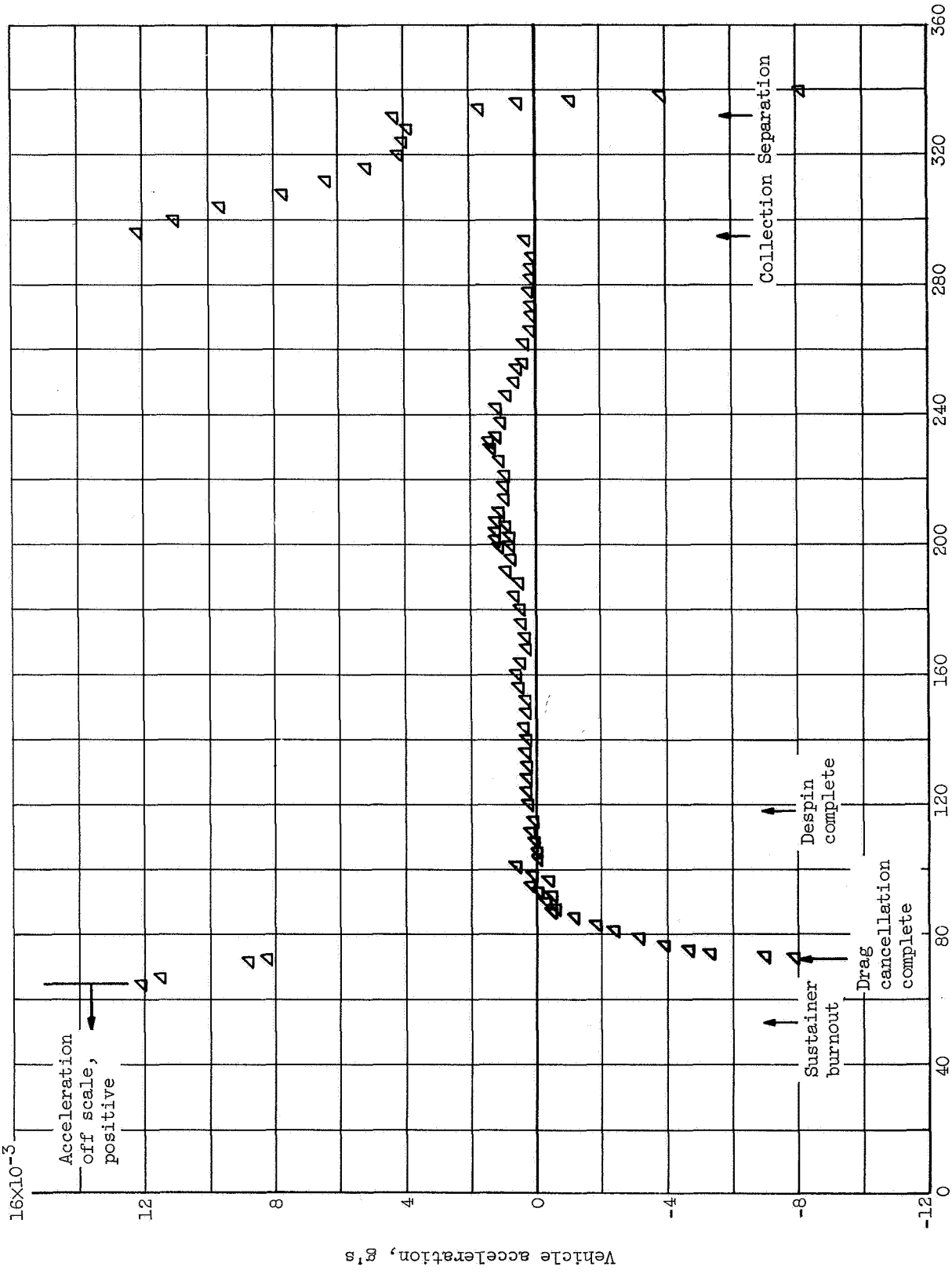

Figure 9. - Rocket-vehicle longitudinal acceleration.

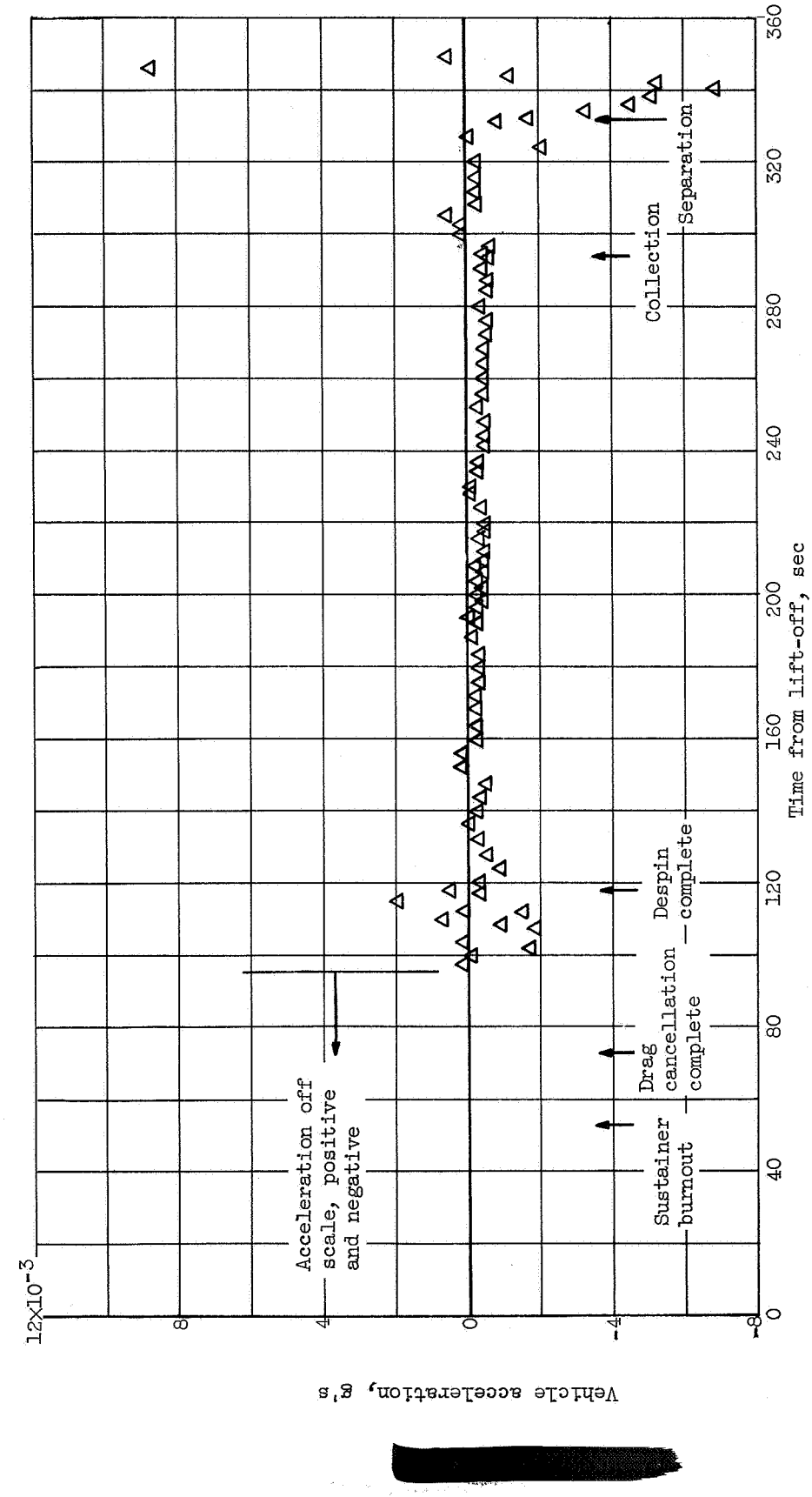

(a) Pitch axis.

Figure 10. - Rocket-vehicle lateral acceleration.

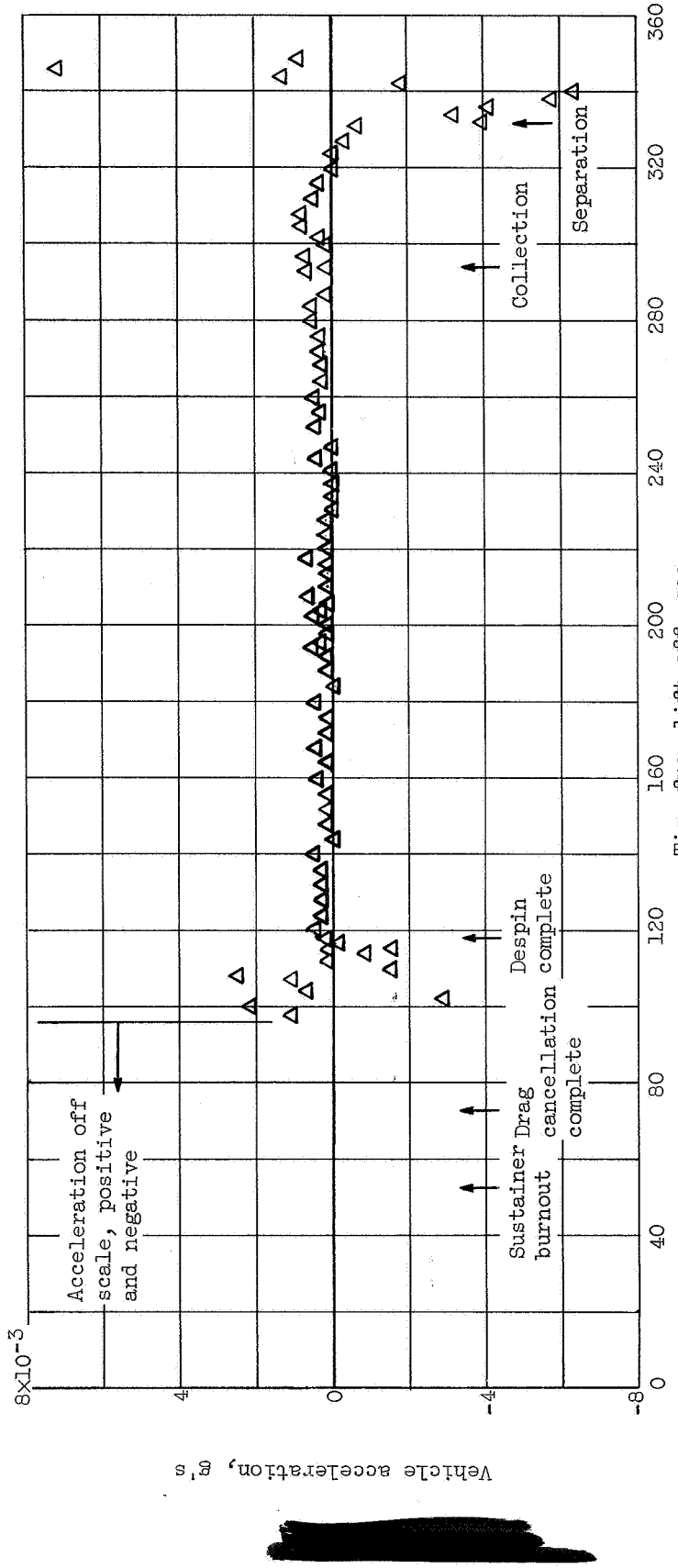

(b) Yaw axis.

Figure 10. - Concluded. Rocket-vehicle lateral acceleration.

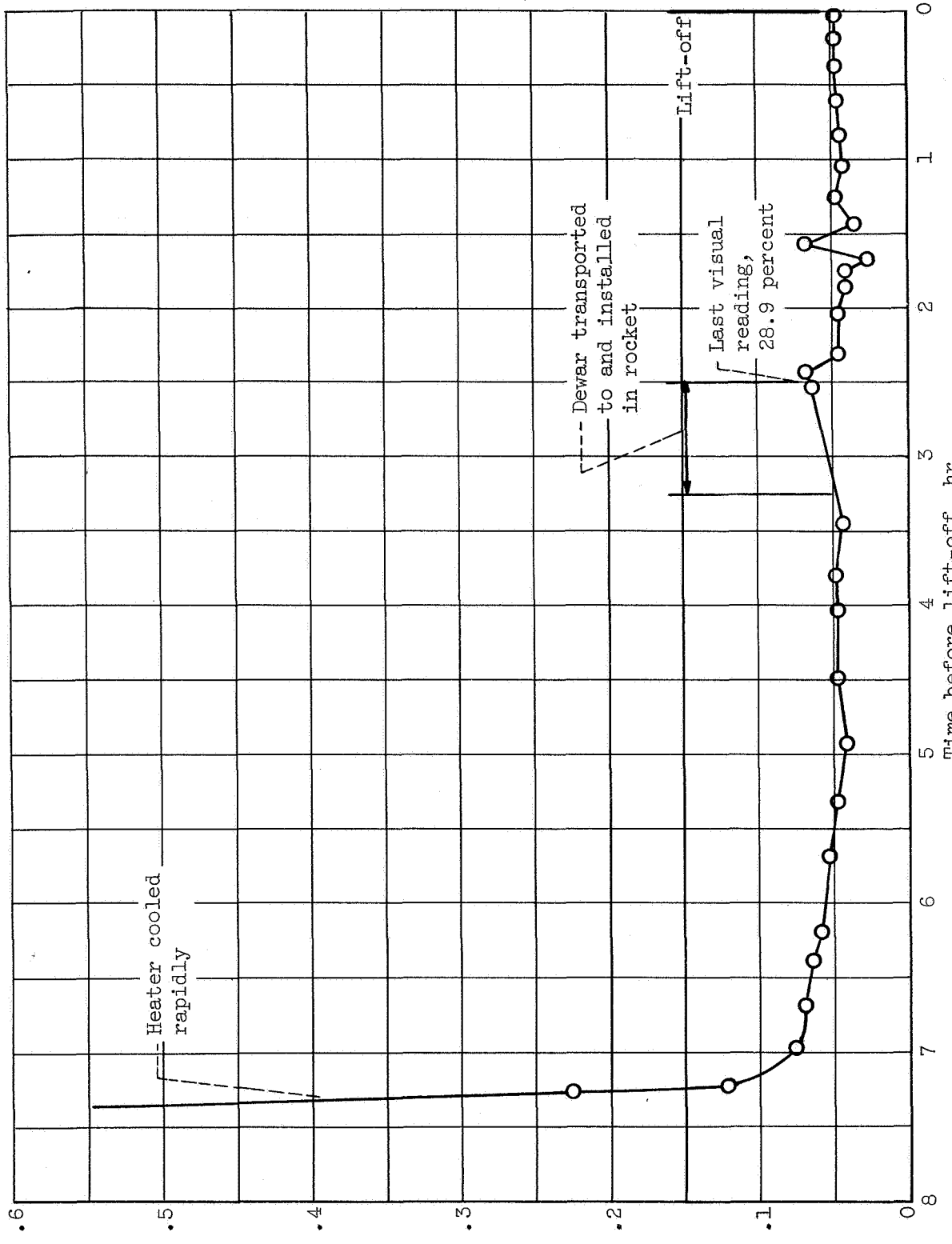

Figure 11. - Hydrogen boiloff before lift-off.

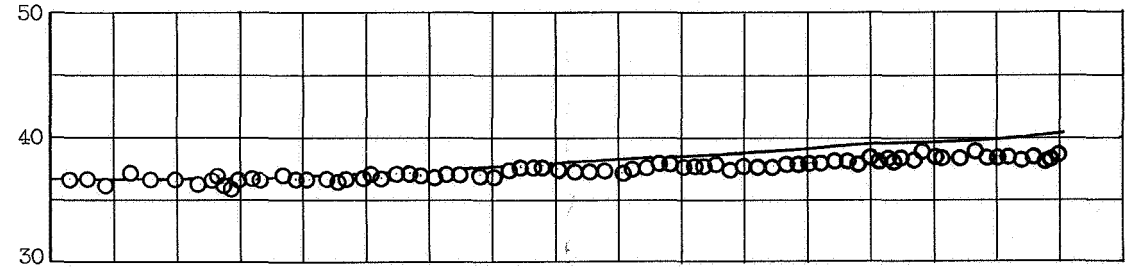

(a) Transducer 4.

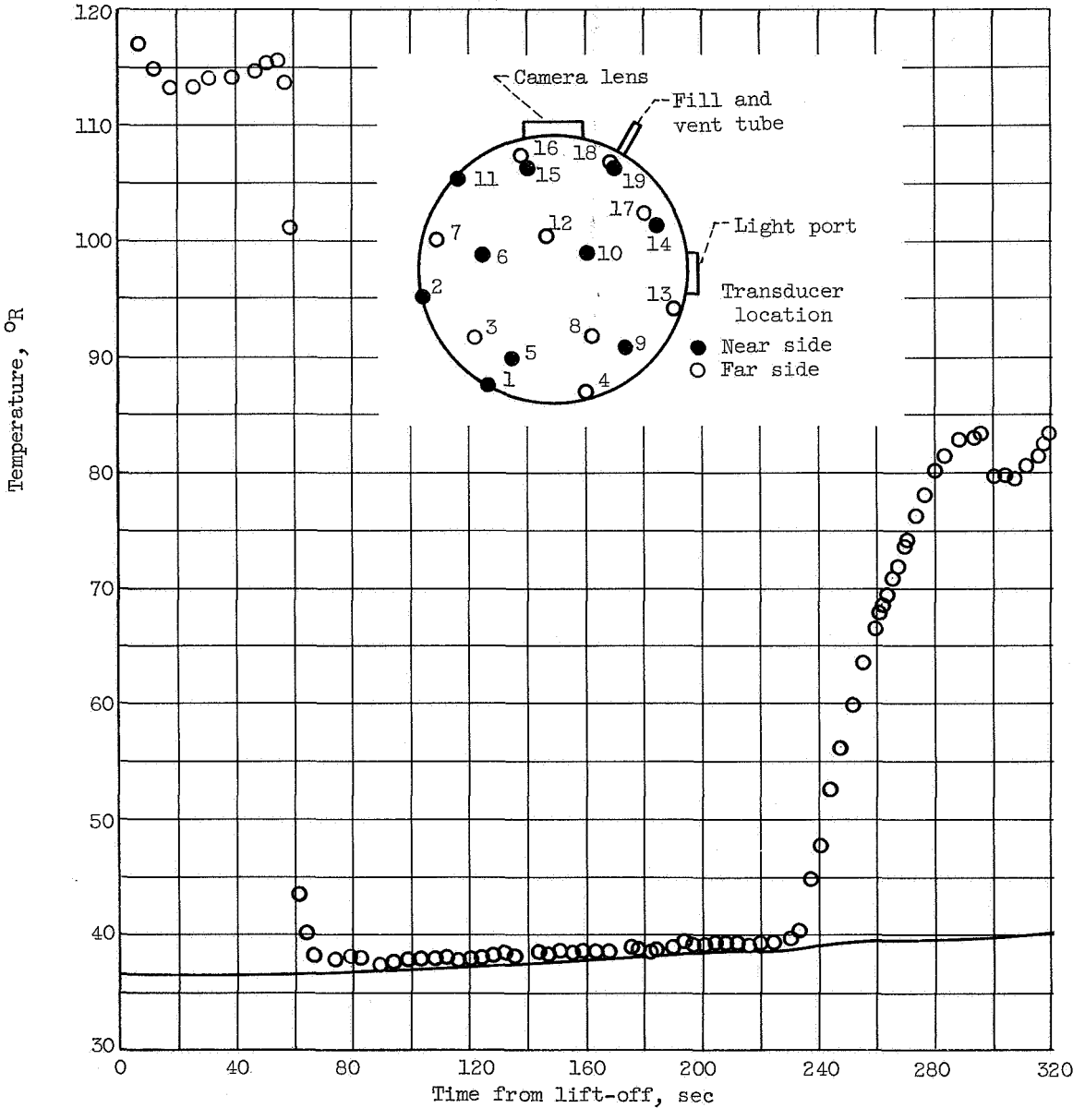

(b) Transducer 16.

Figure 12. - Hydrogen-tank wall-temperature histories measured by transducers 4 and 16.

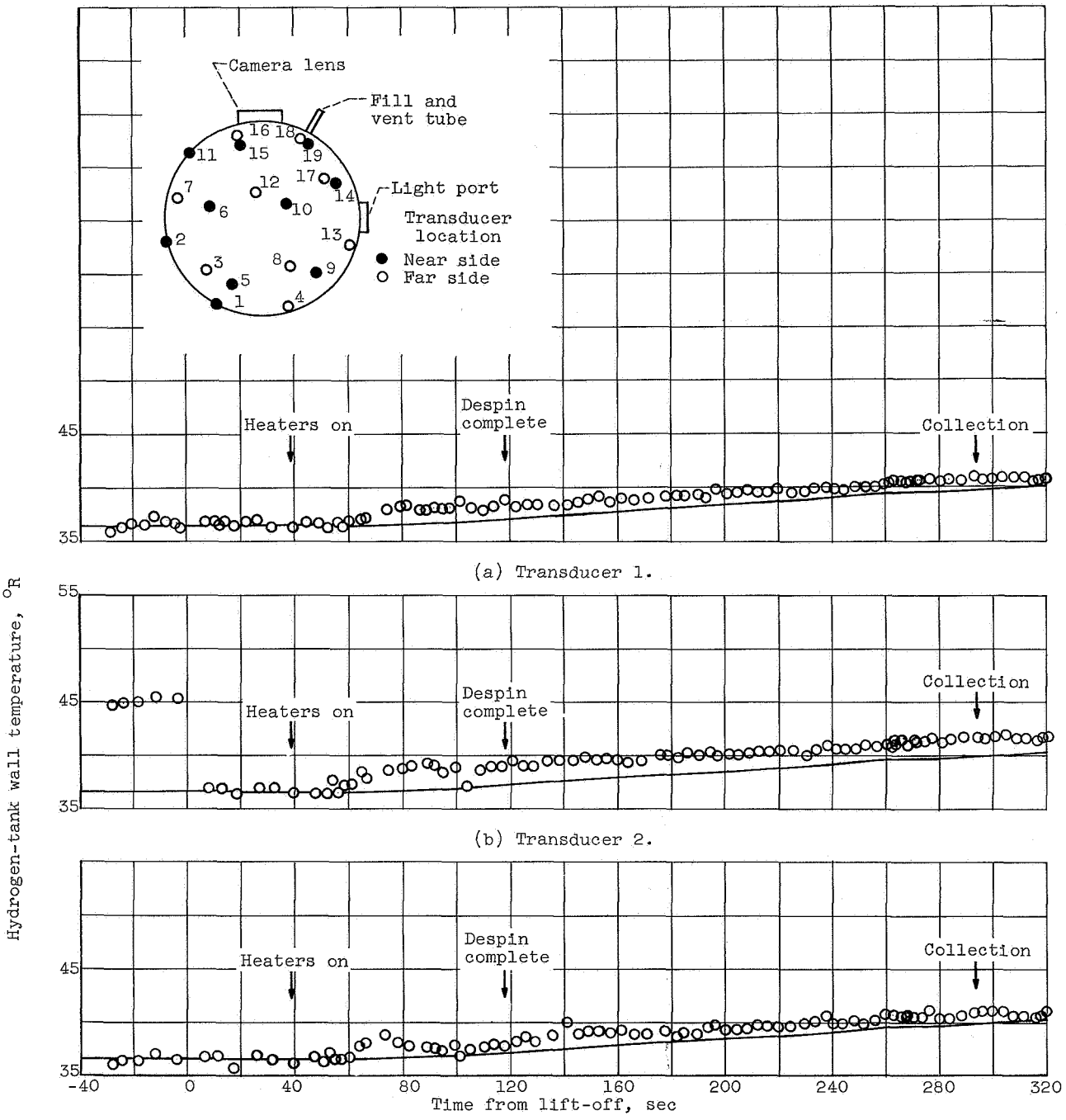

Figure 13. - Hydrogen-tank wall-temperature histories measured by various transducers.

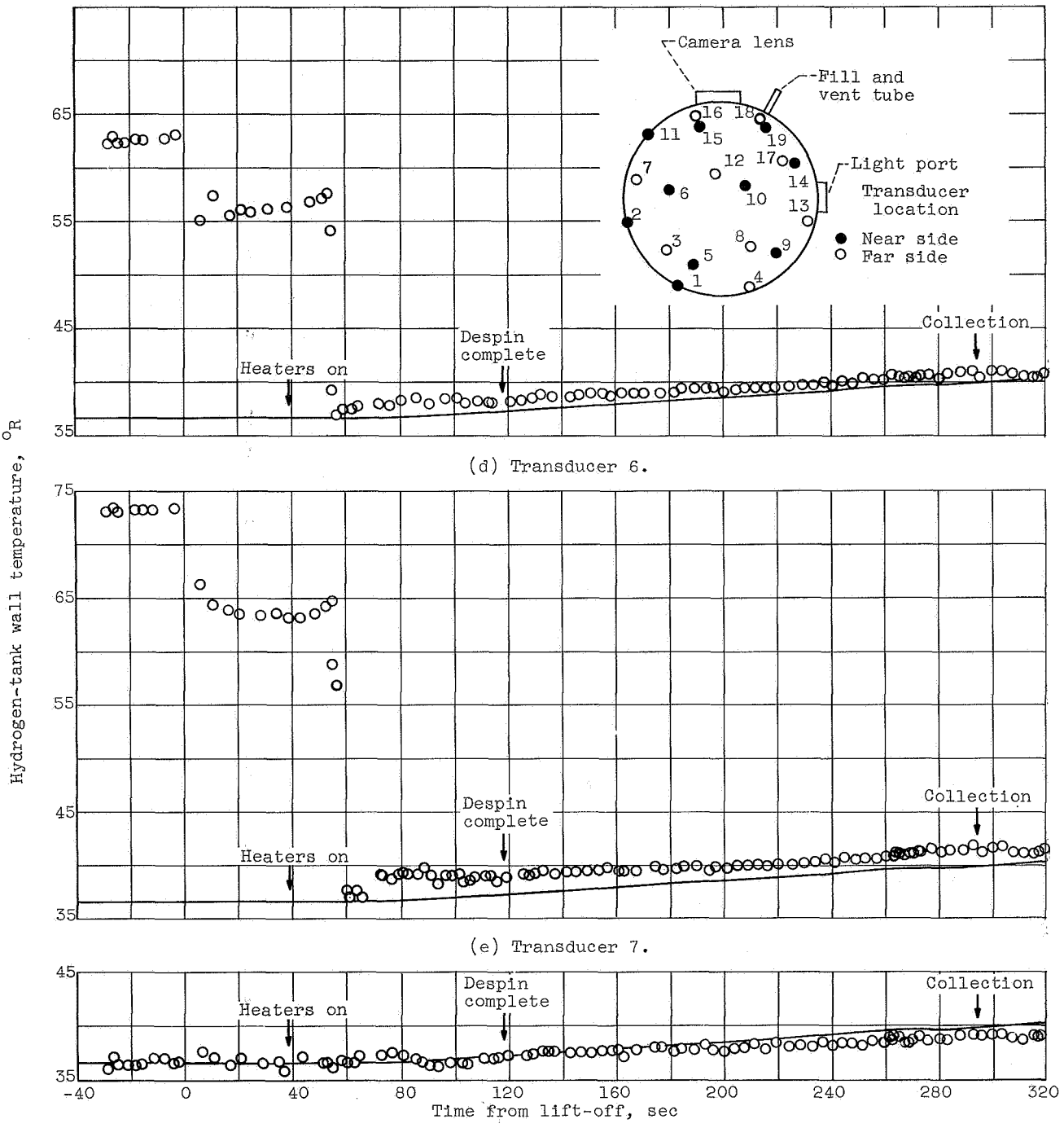

(d) Transducer 6.

(e) Transducer 7.

(f) Transducer 8.

Figure 13. - Continued. Hydrogen-tank wall-temperature histories measured by various transducers.

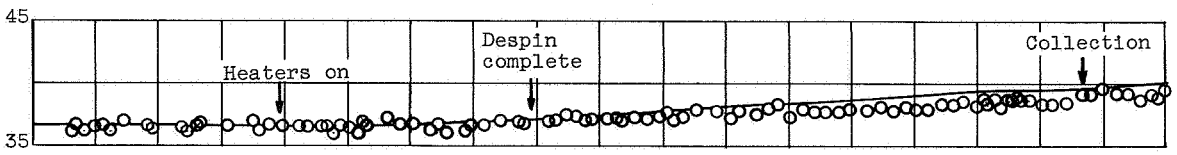

(g) Transducer 9.

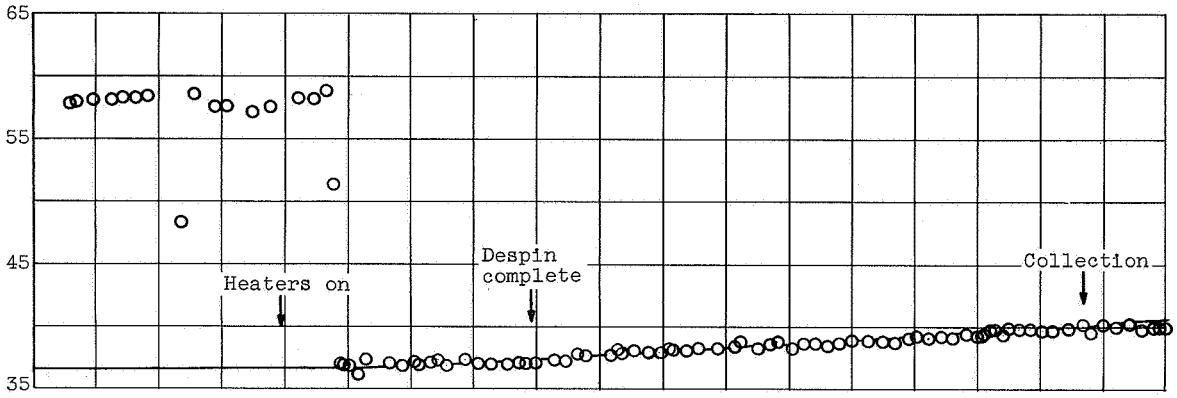

(h) Transducer 10.

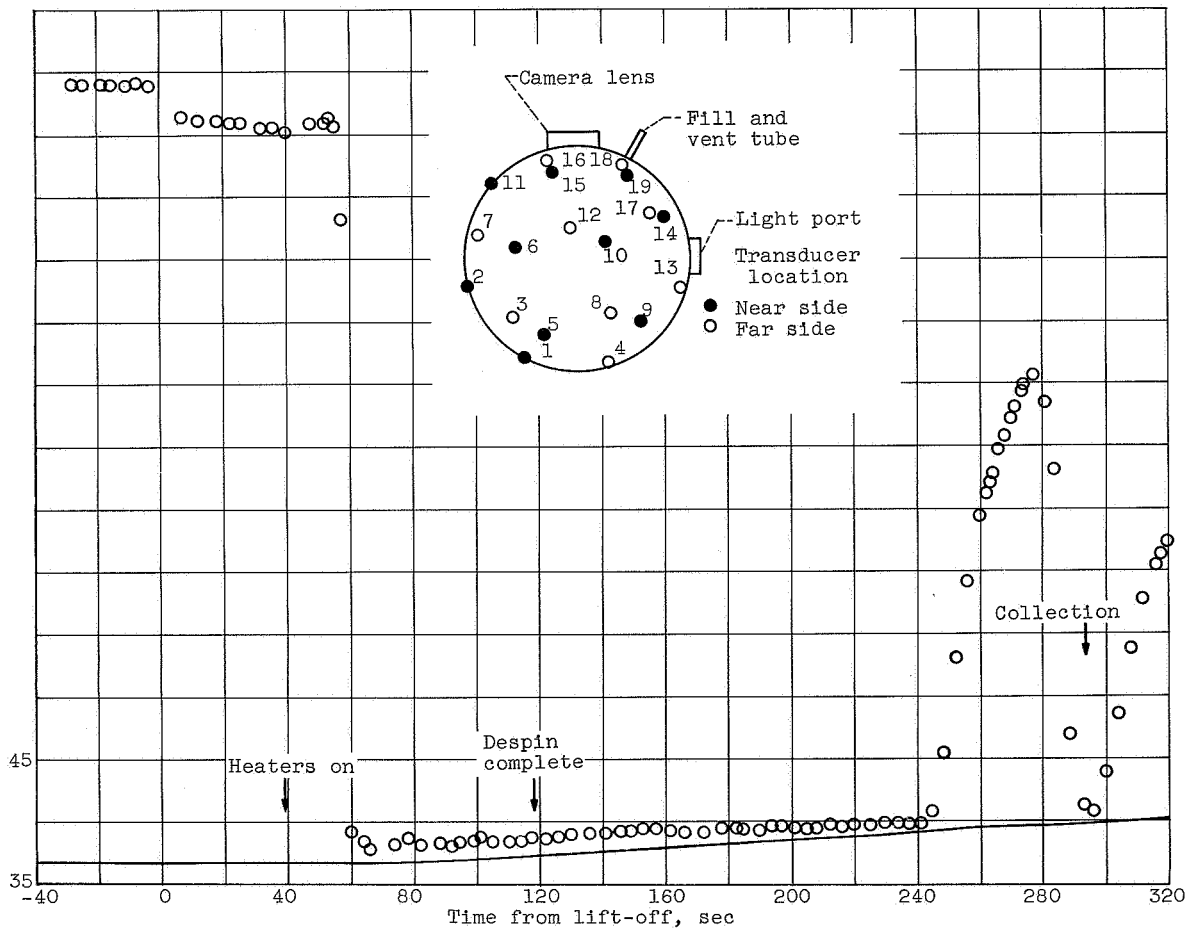

(i) Transducer 11.

Figure 13. - Continued. Hydrogen-tank wall-temperature histories measured by various transducers.

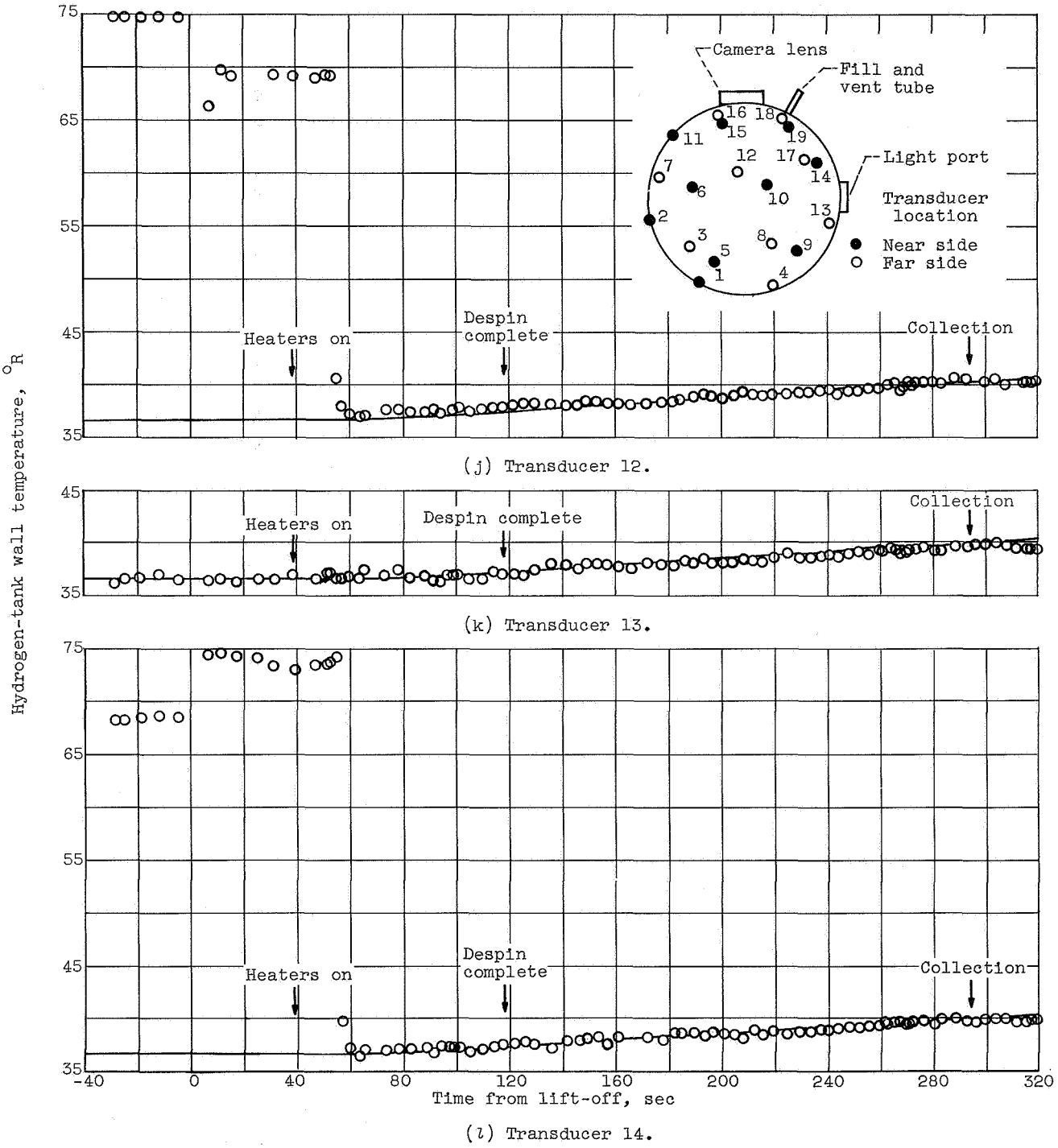

Figure 13. - Continued. Hydrogen-tank wall-temperature histories measured by various transducers.

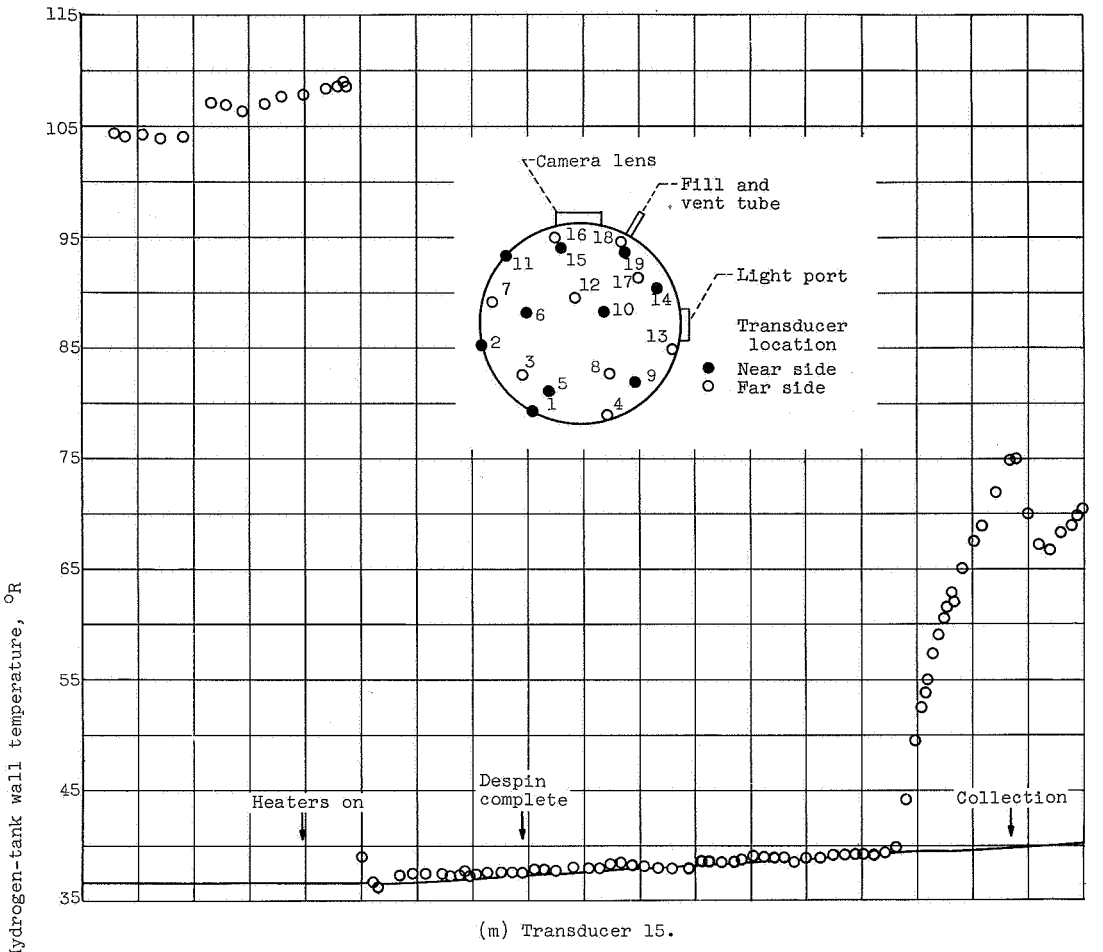

(m) Transducer 15.

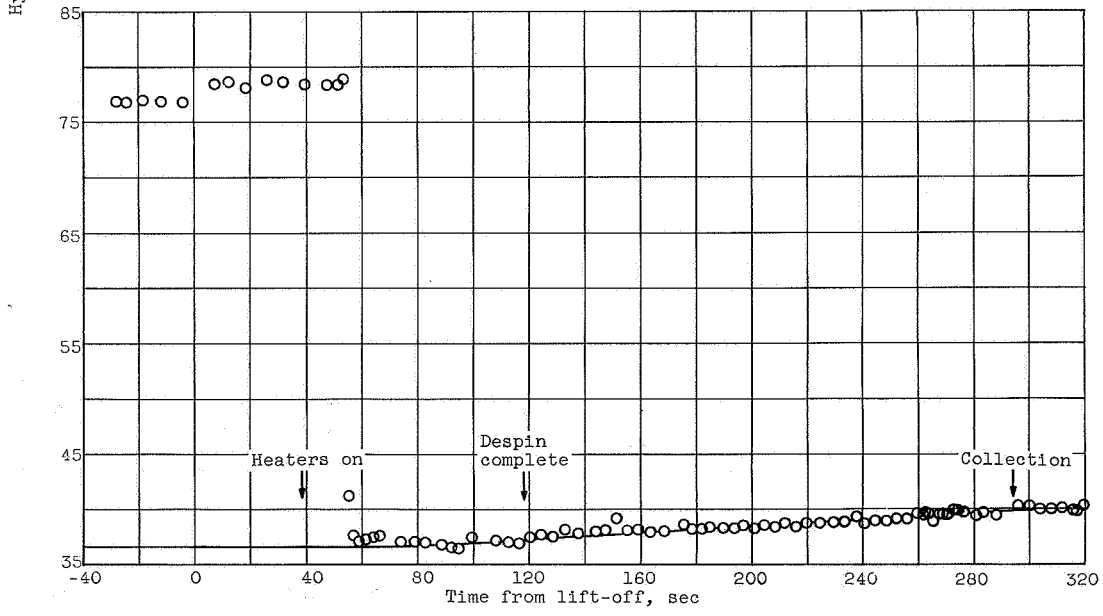

(n) Transducer 17.

Figure 13. - Continued. Hydrogen-tank wall-temperature histories measured by various transducers.

CONFIDENTIAL

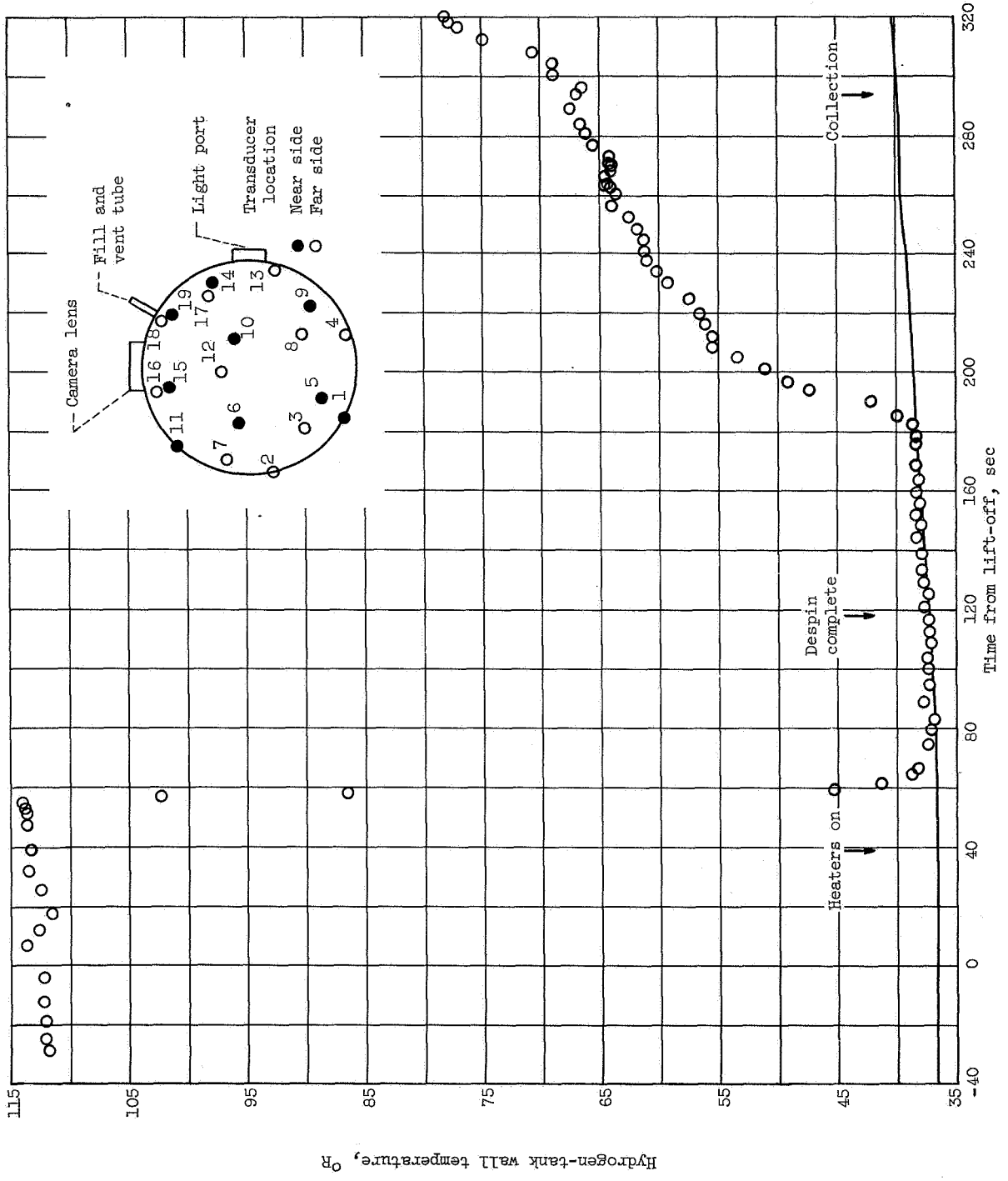

(o) Transducer 18.

Figure 13. - Continued. Hydrogen-tank wall-temperature histories measured by various transducers.

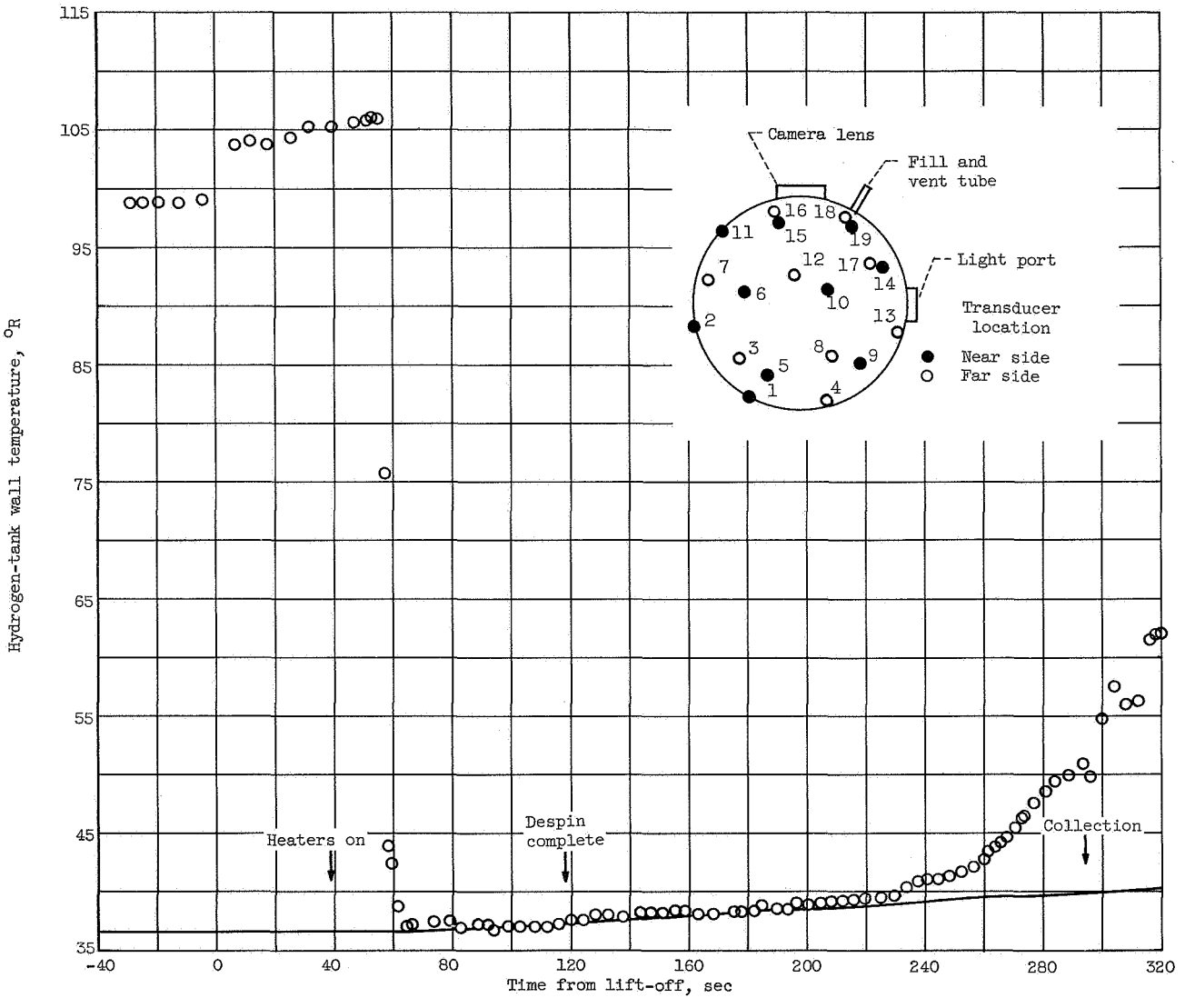

(p) Transducer 19.

Figure 13. - Concluded. Hydrogen-tank wall-temperature histories measured by various transducers.

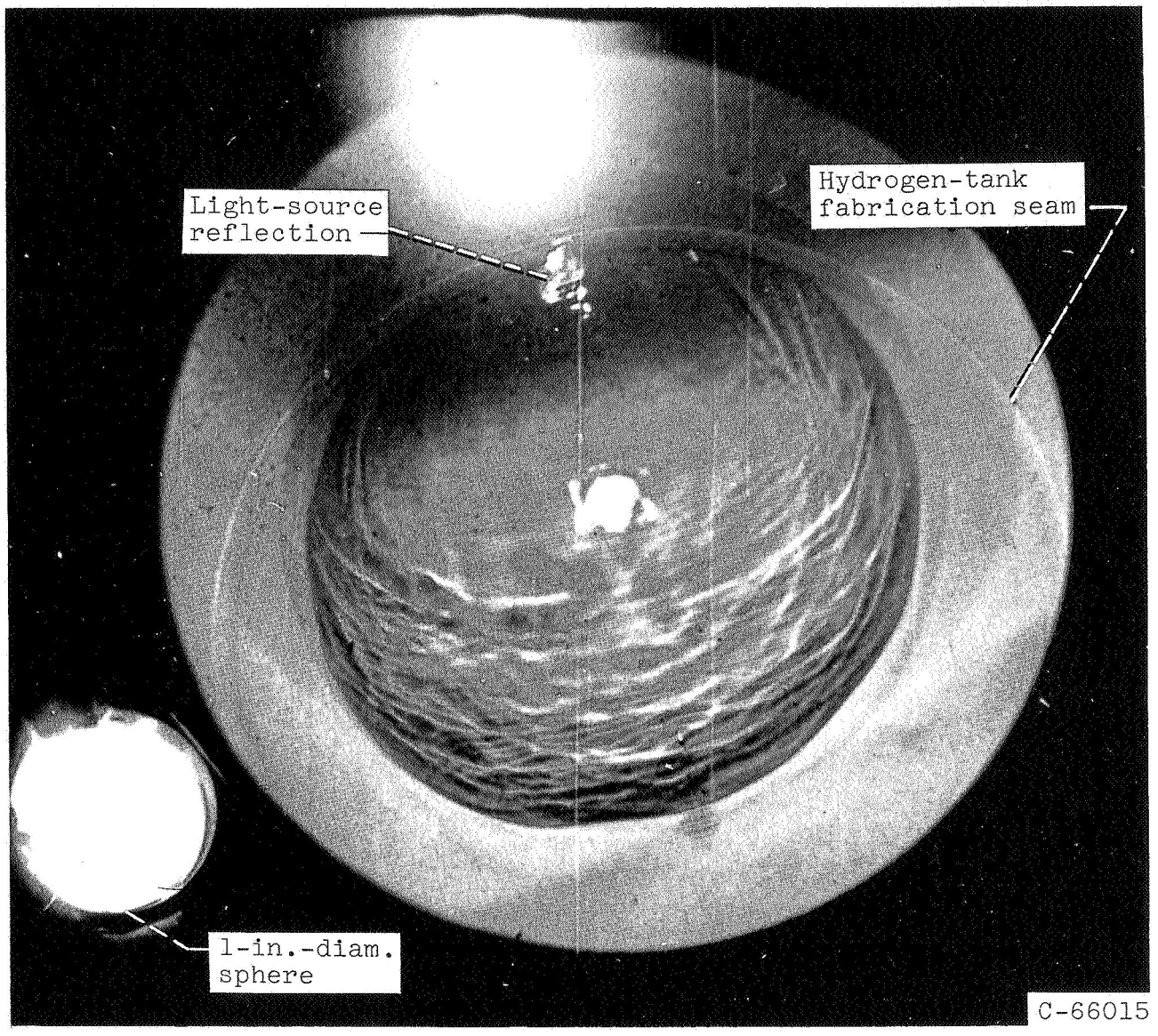

41.3 sec

(a) Configuration during sustainer firing.

Figure 14. - Liquid hydrogen at various flight times.

CONFIDENTIAL

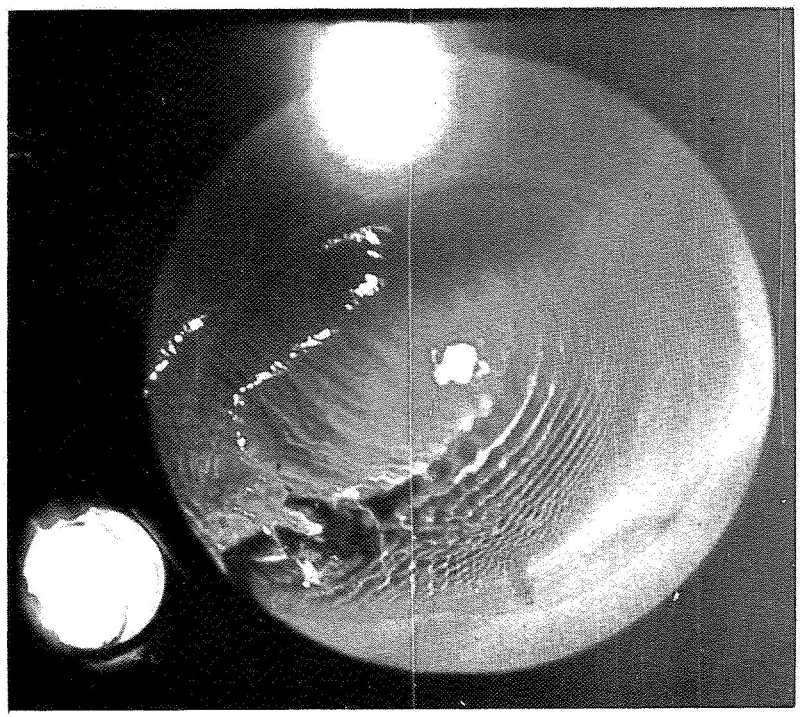

Before drop in upper wall temperature, 55.4 sec

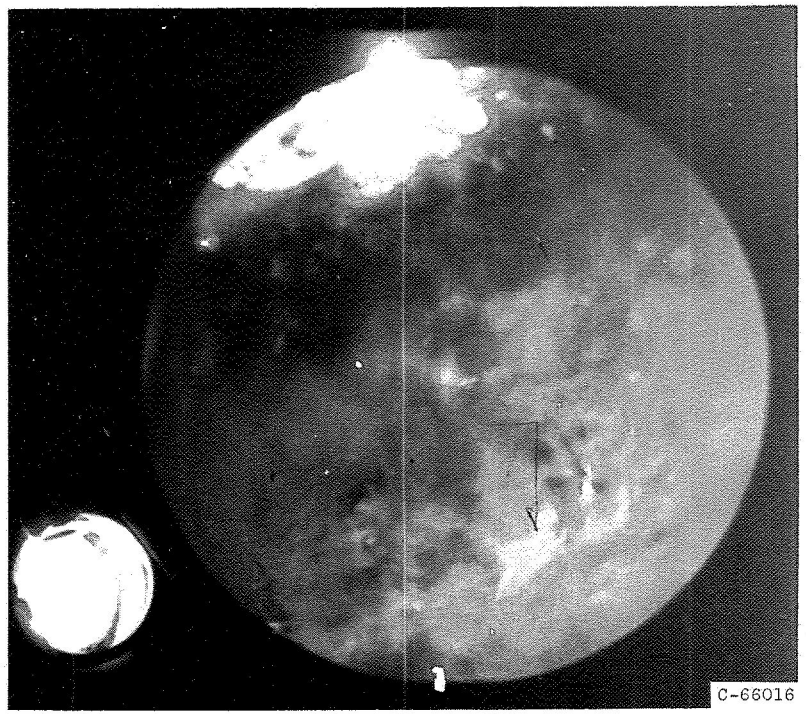

After wall temperature began to drop, 58.5 sec

(b) Fluid assuming zero-gravity configuration after burnout.

Figure 14. - Continued. Liquid hydrogen at various flight times.

CONFIDENTIAL

CONFIDENTIAL

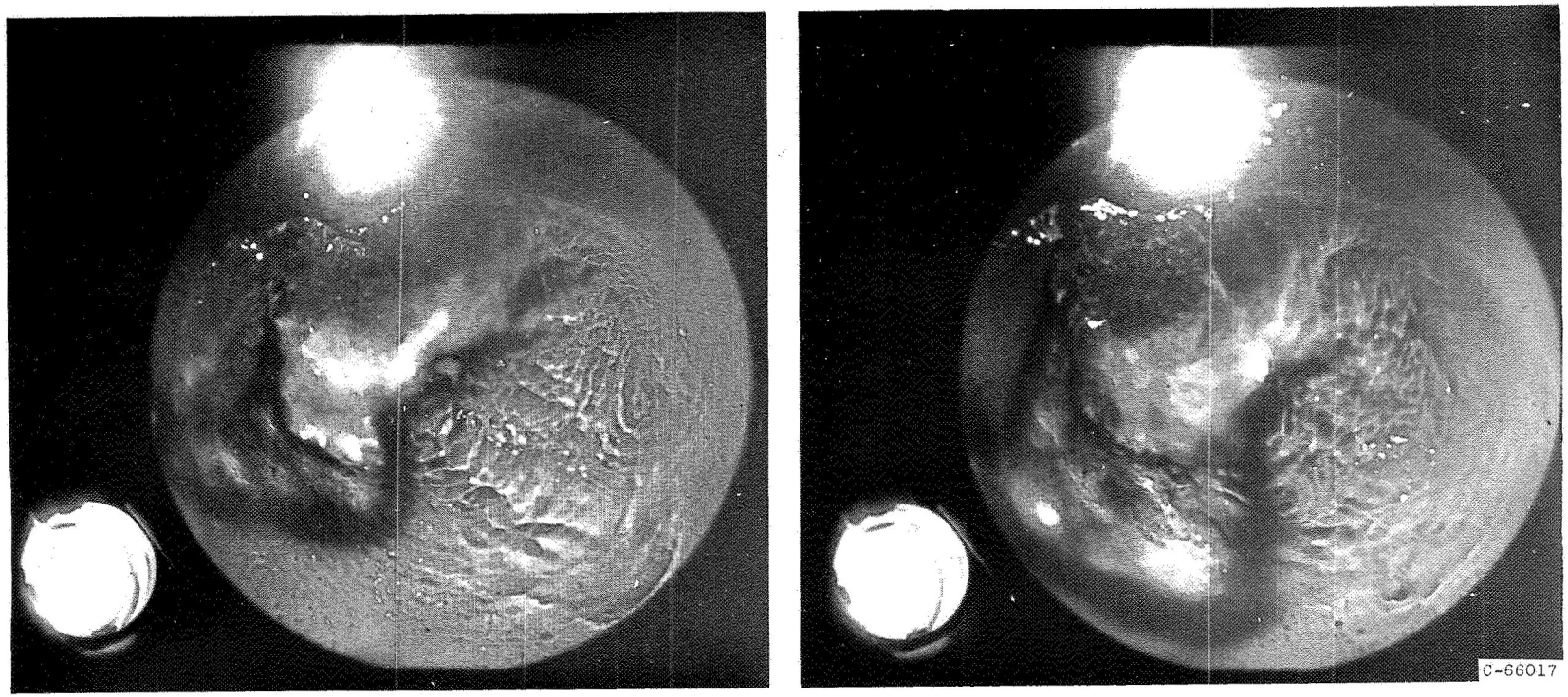

62.9 sec

63.1 sec

(c) Counterclockwise liquid swirling during drag-cancellation operation.

Figure 14. - Continued. Liquid hydrogen at various flight times.

CONFIDENTIAL

CONFIDENTIAL

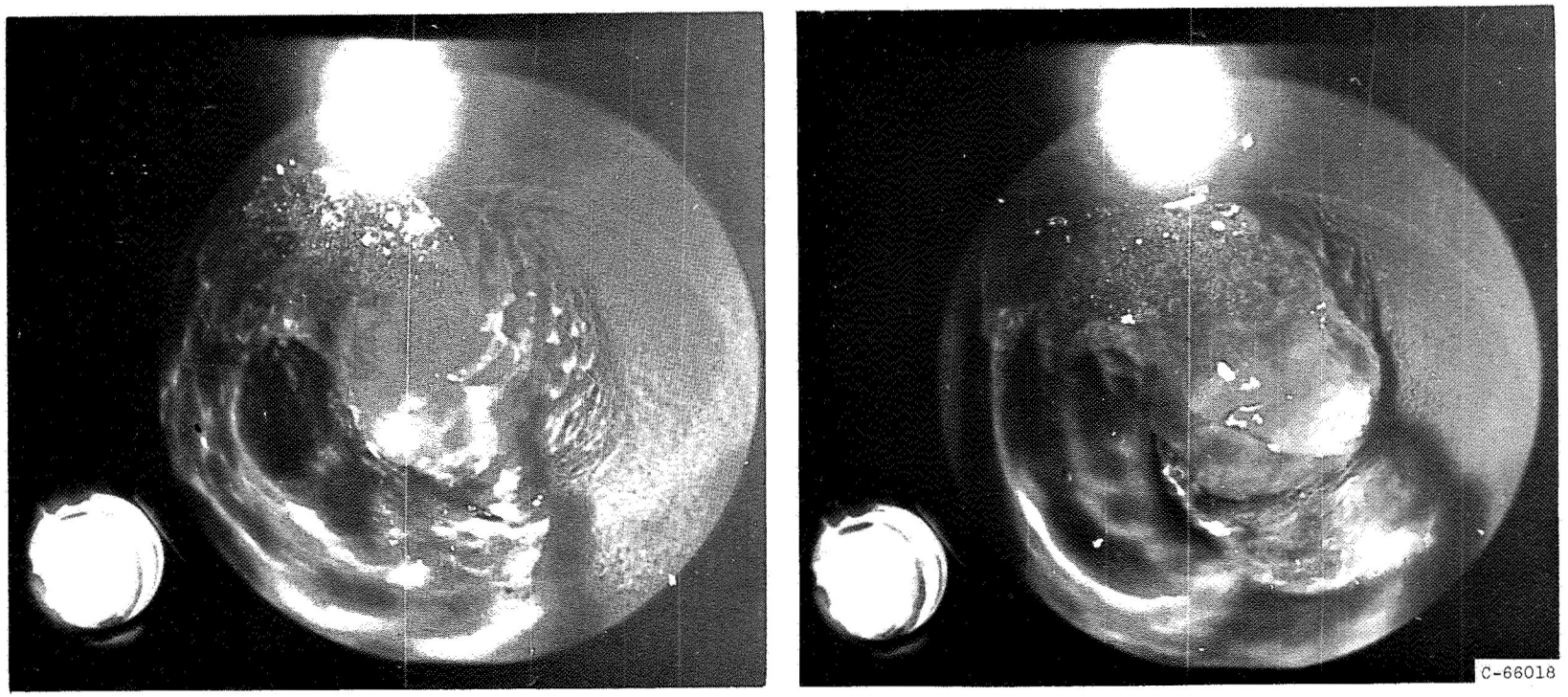

63.5 sec

63.9 sec

(c) Concluded. Counterclockwise liquid swirling during drag-cancellation operation.

Figure 14. - Continued. Liquid hydrogen at various flight times.

CONFIDENTIAL

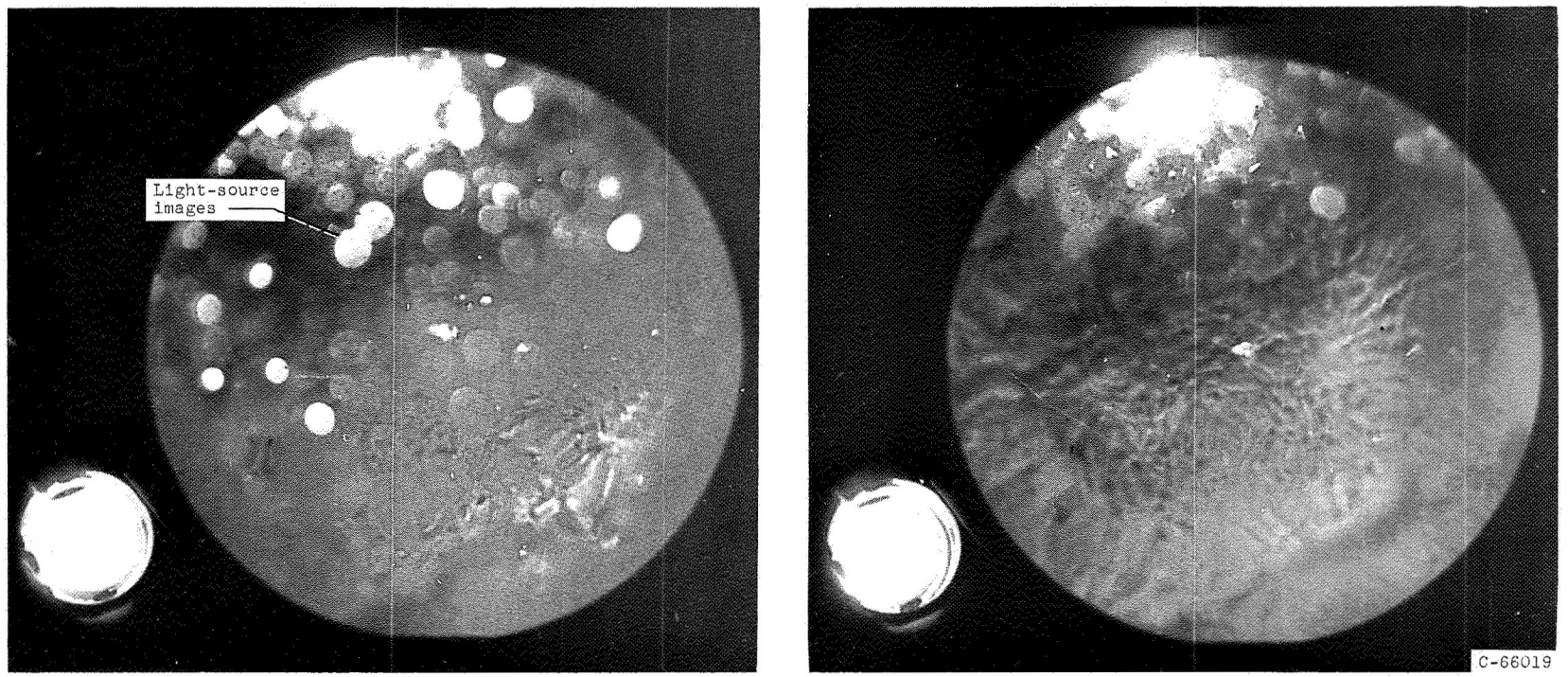

98.5 sec 114.3 sec

(d) Configuration during despin.

Figure 14. - Continued. Liquid hydrogen at various flight times.

CONFIDENTIAL

CONFIDENTIAL

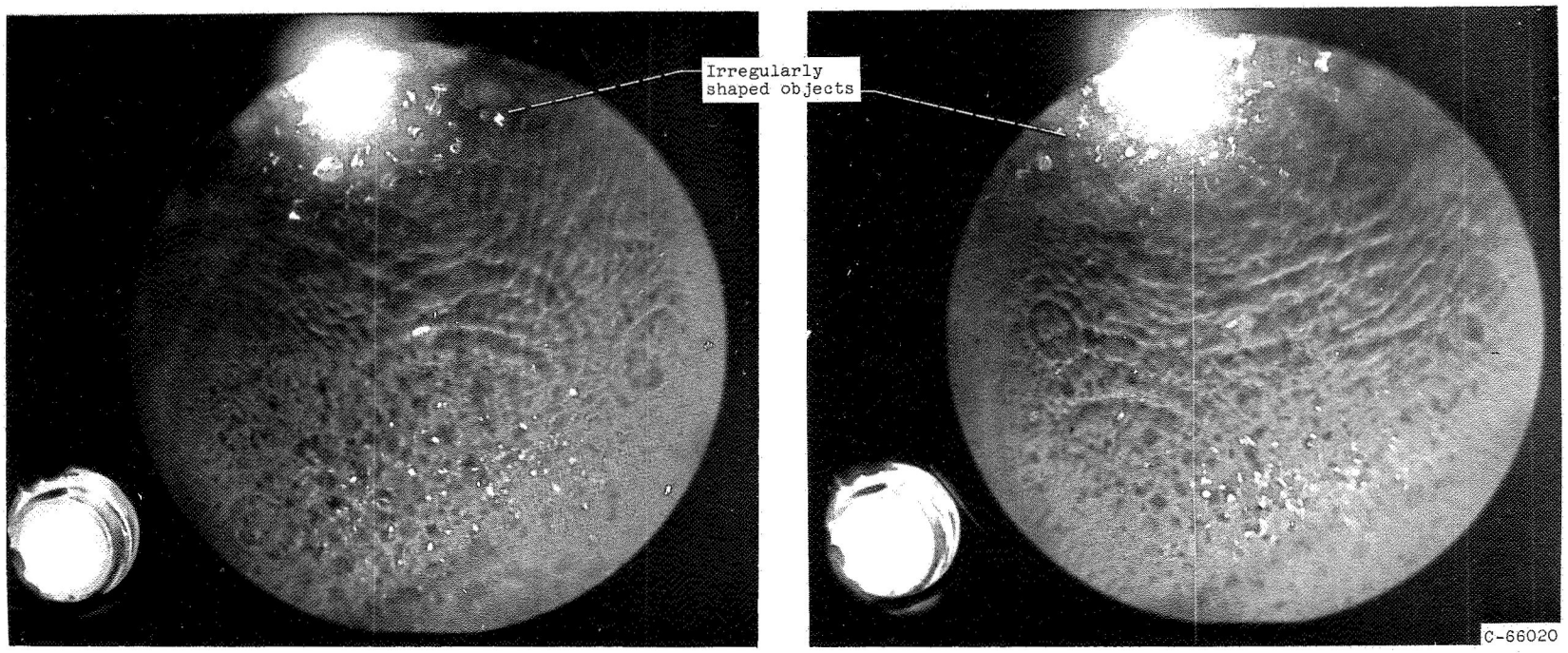

137.7 sec 140.0 sec

(e) Configuration shortly after despin.

Figure 14. - Continued. Liquid hydrogen at various flight times.

CONFIDENTIAL

CONFIDENTIAL

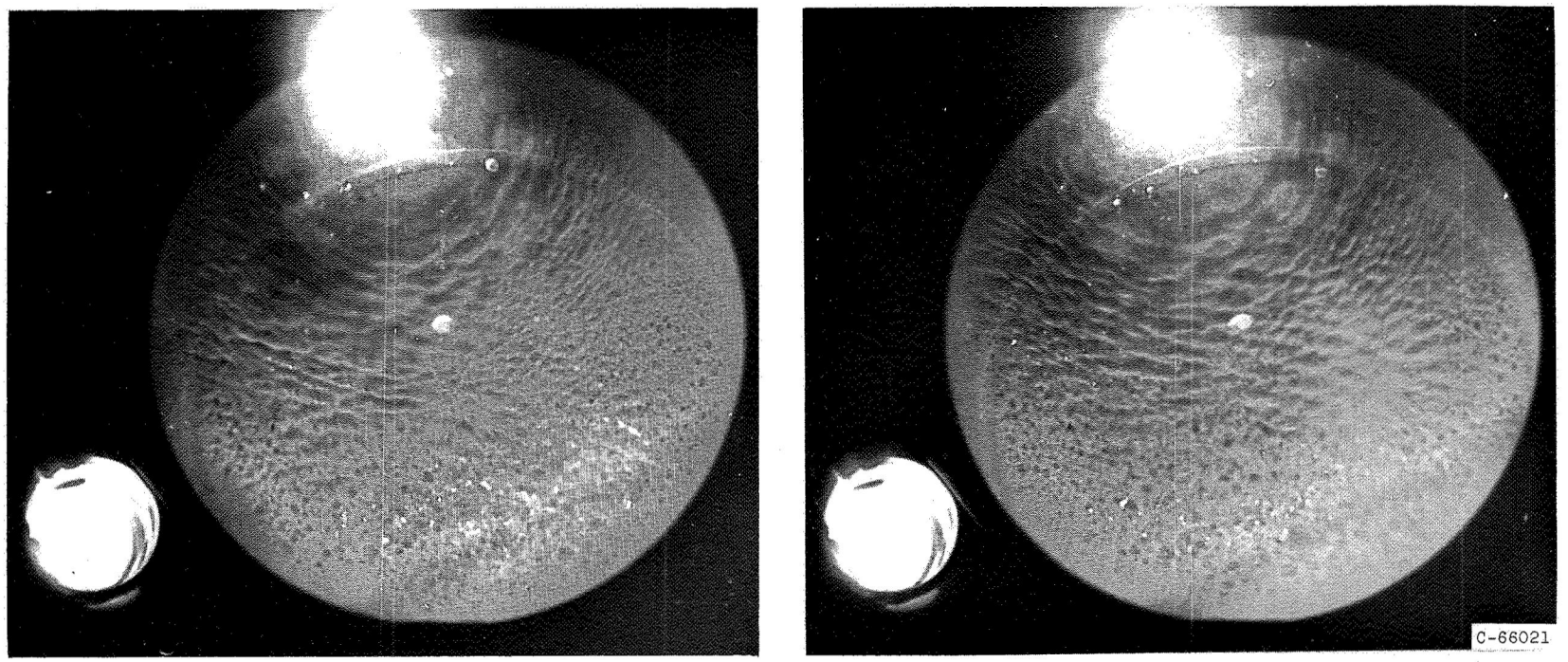

164.4 sec

164.6 sec

(f) Appearance of bubbles.

Figure 14. - Continued. Liquid hydrogen at various flight times.

CONFIDENTIAL

164.8 sec

165.0 sec

(f) Concluded. Appearance of bubbles.

Figure 14. - Continued. Liquid hydrogen at various flight times.

CONFIDENTIAL

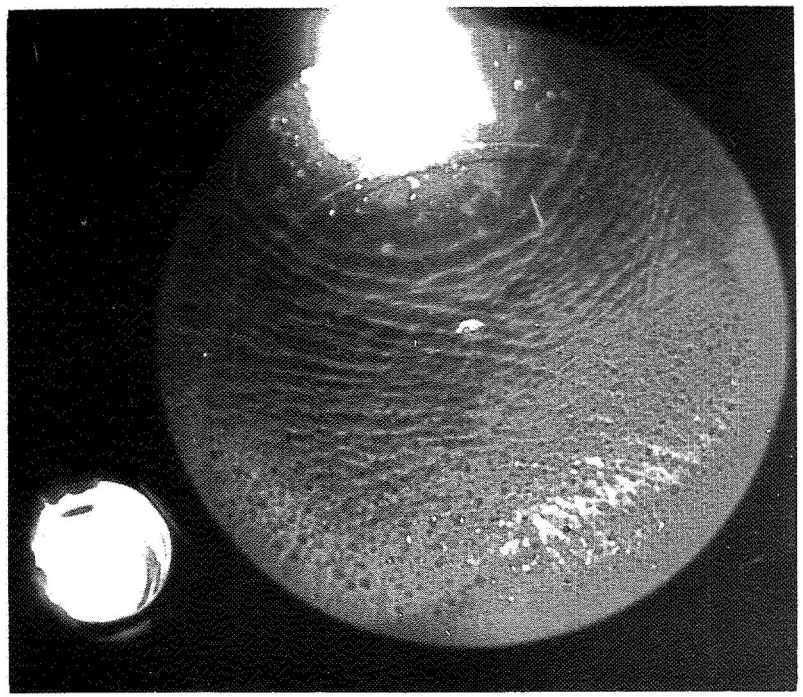

274.2 sec

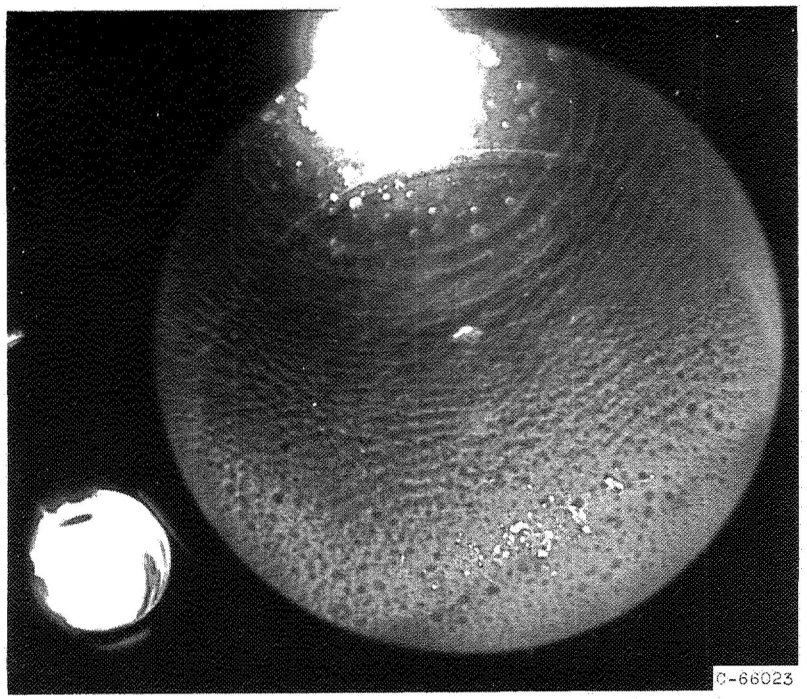

276.7 sec

(g) Increased numbers and sizes of bubbles near end of weightless period.

Figure 14. - Continued. Liquid hydrogen at various flight times.

CONFIDENTIAL

CONFIDENTIAL

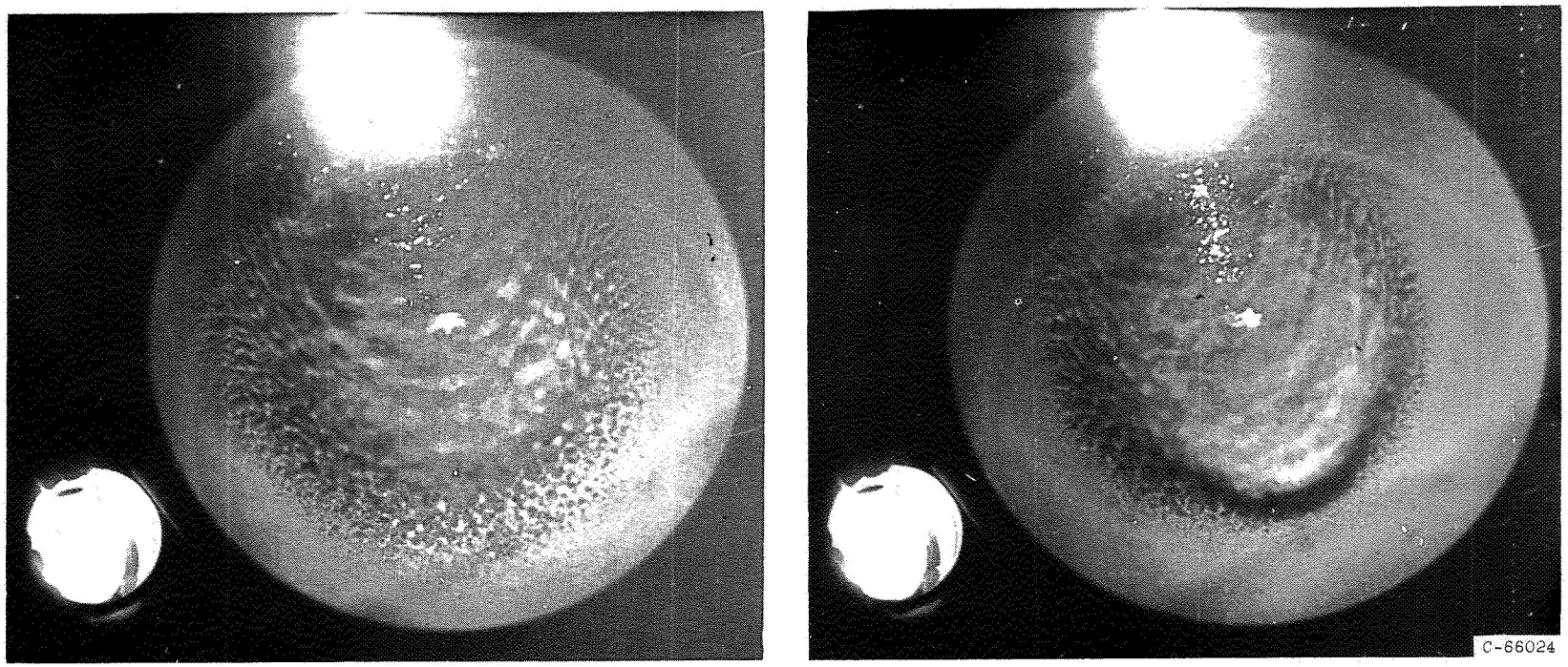

294.3 sec 294.5 sec

(h) Effect of collection thrust on liquid.

Figure 14. - Continued. Liquid hydrogen at various flight times.

CONFIDENTIAL

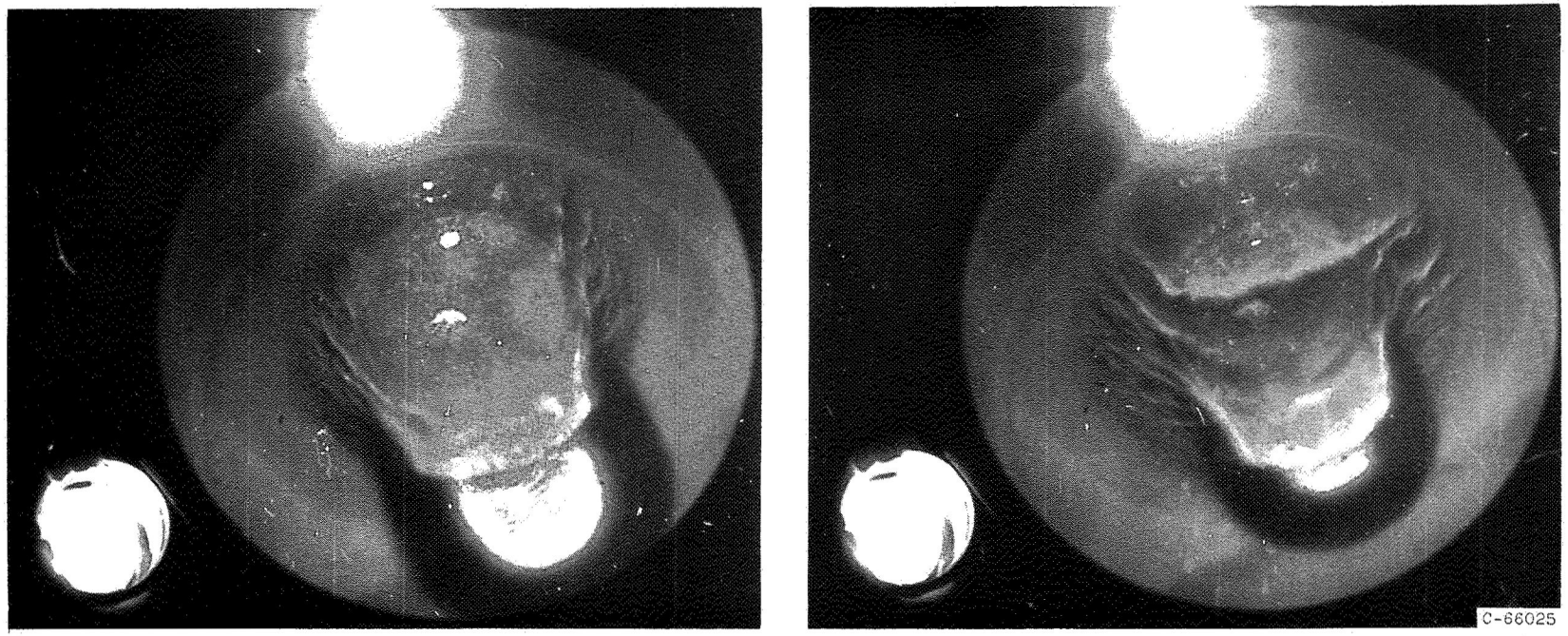

295.7 sec

296.1 sec

(h) Continued. Effect of collection thrust on liquid.

Figure 14. - Continued. Liquid hydrogen at various flight times.

CONFIDENTIAL

CONFIDENTIAL

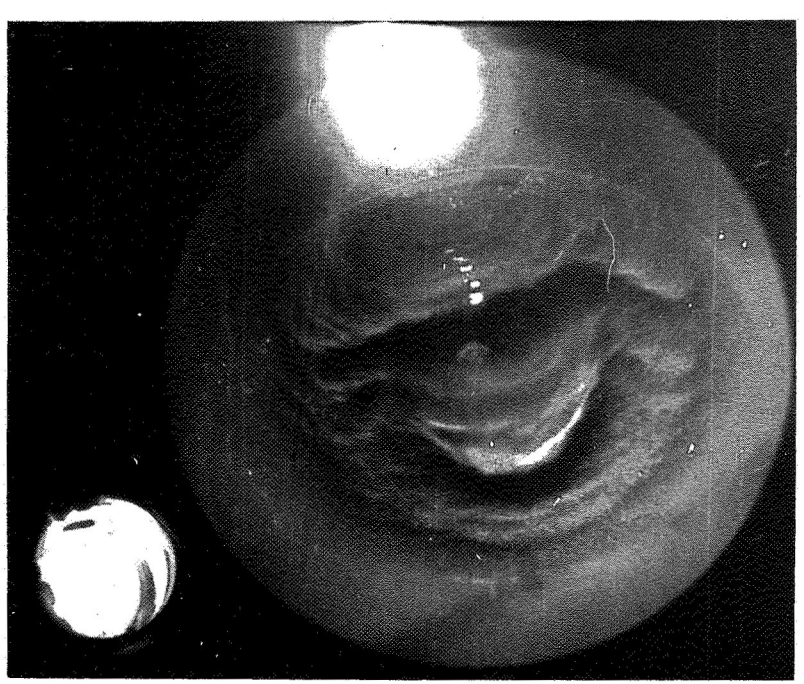

296.5 sec

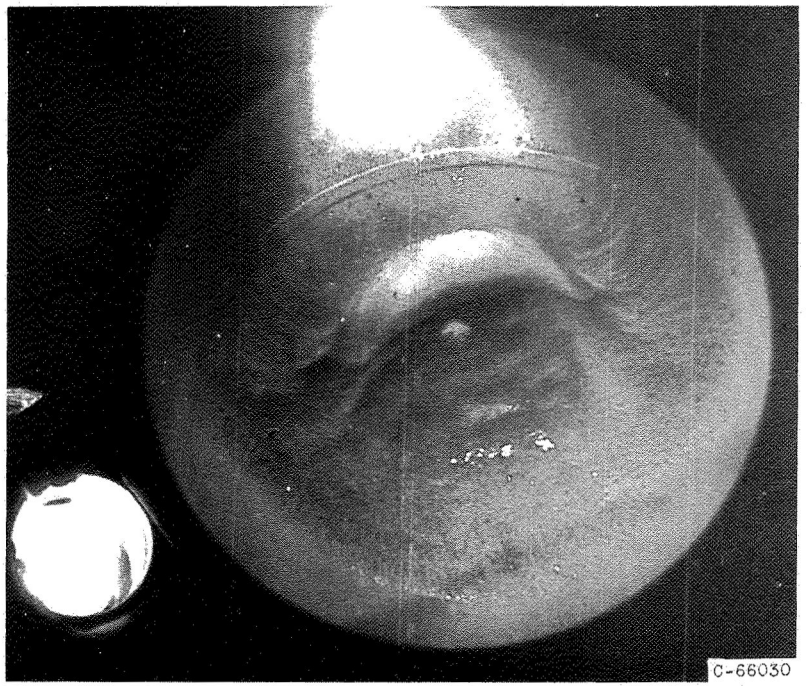

297.1 sec

(h) Concluded. Effect of collection thrust on liquid.

Figure 14. - Concluded. Liquid hydrogen at various flight times.

CONFIDENTIAL

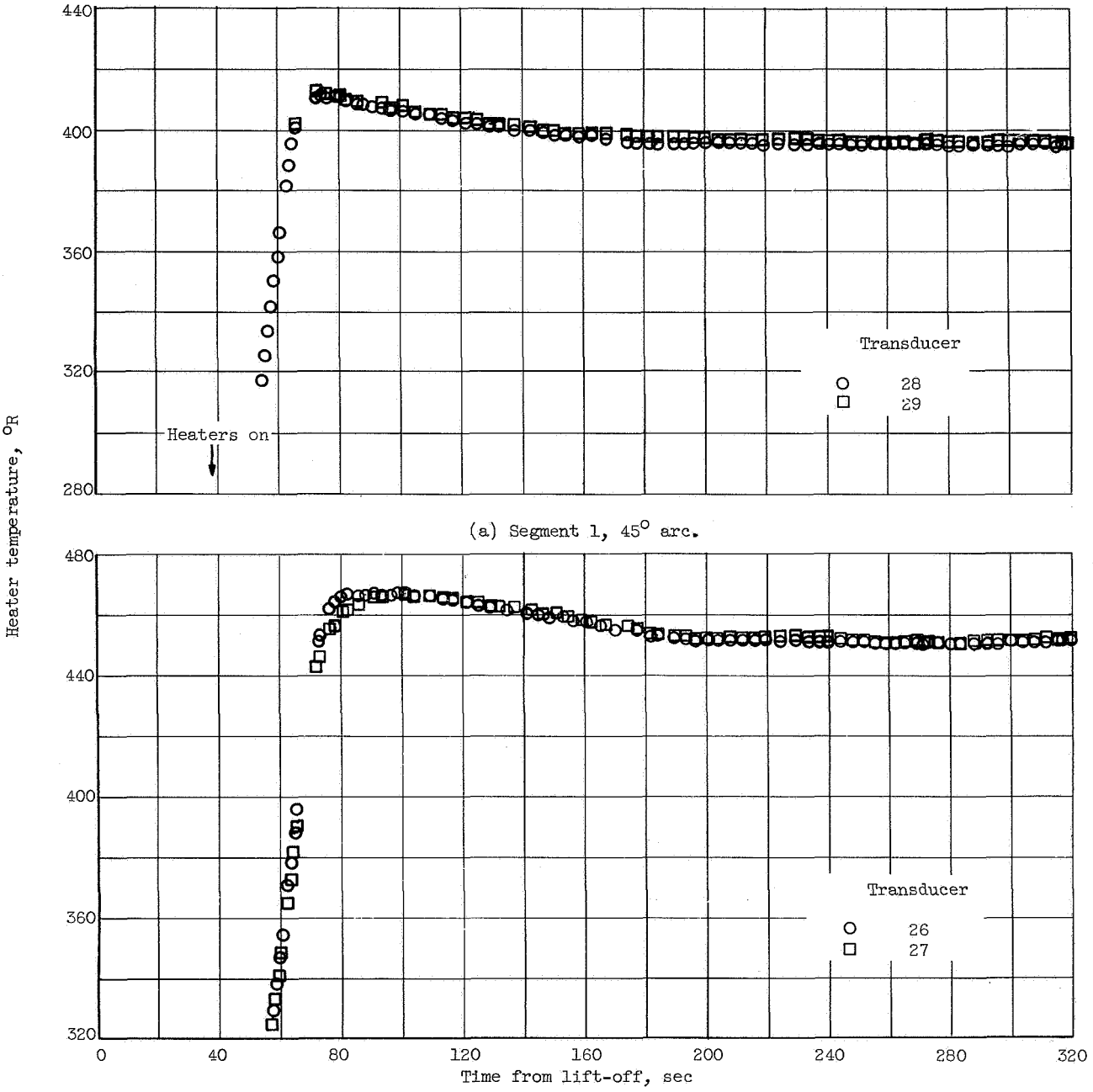

(a) Segment 1, 45° arc.

(b) Segment 2, 90° arc.

Figure 15. - Temperature as function of time for various heater segments.

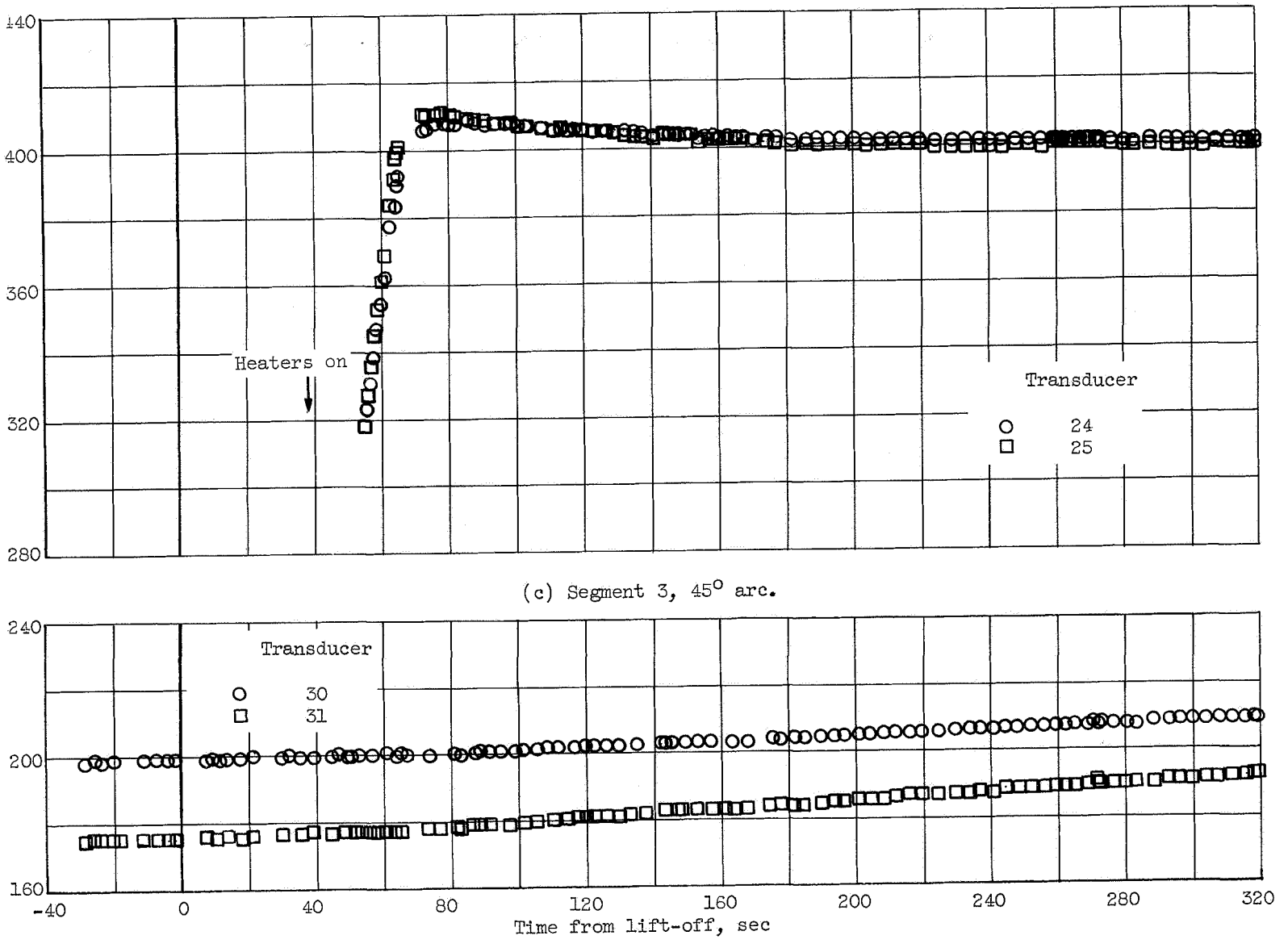

(c) Segment 3, 45° arc.

(d) Segment 4, (dummy segment), 180° arc.

Figure 15. - Concluded. Temperature as function of time for various heater segments.

CONFIDENTIAL

DECLASSIFIED

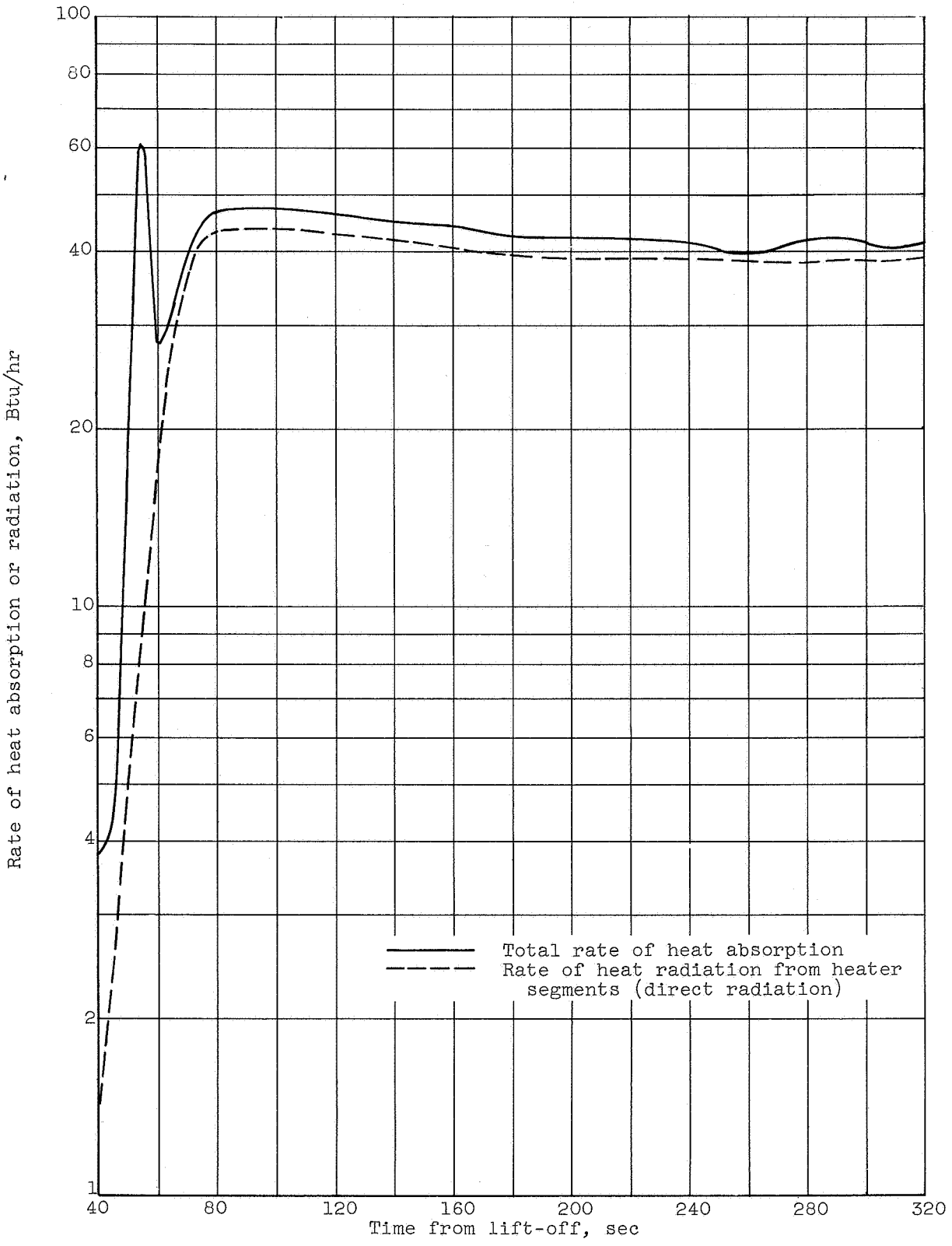

Figure 16. - Rate of heat absorption by hydrogen.

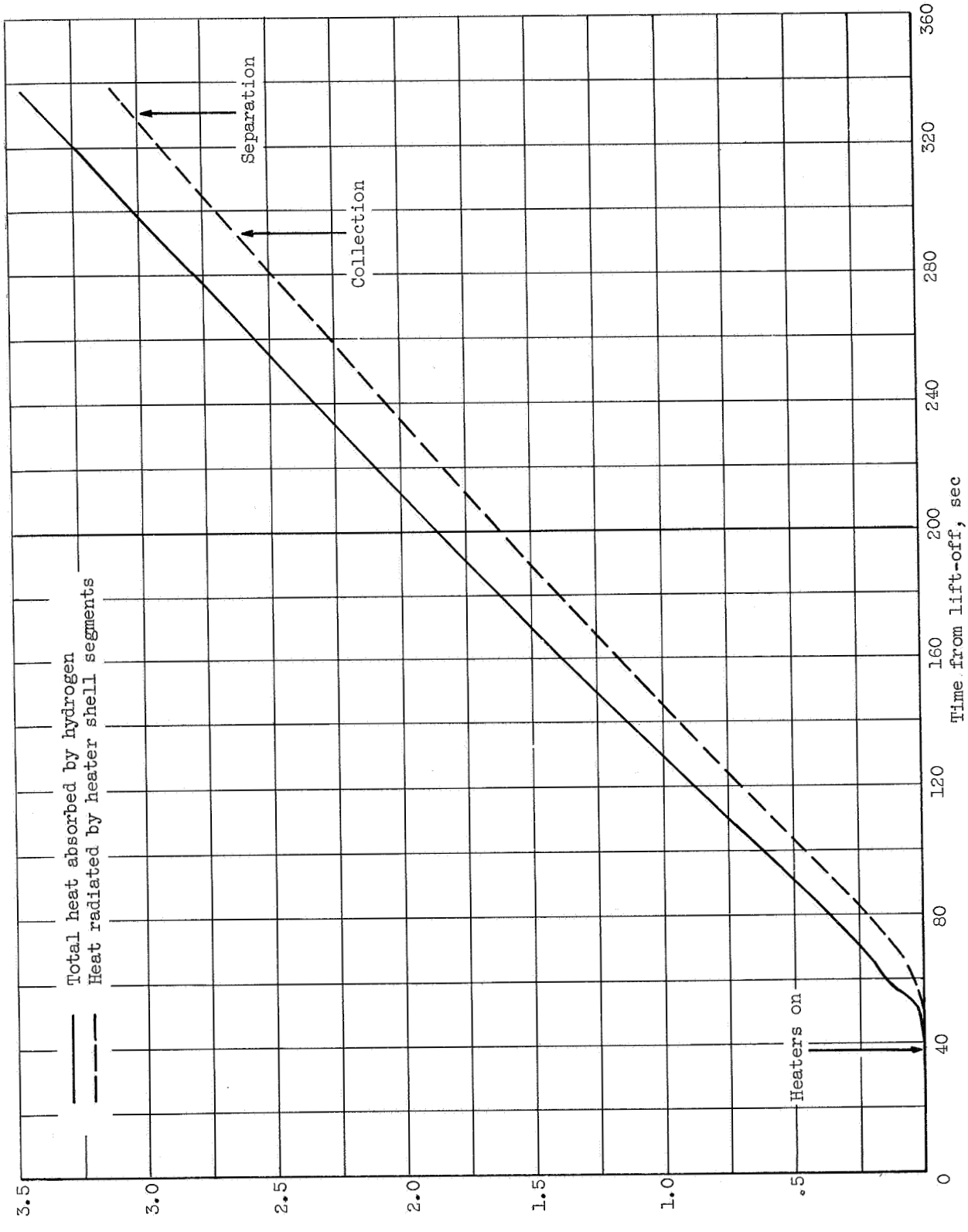

Figure 17. - Heat absorbed by hydrogen during flight.

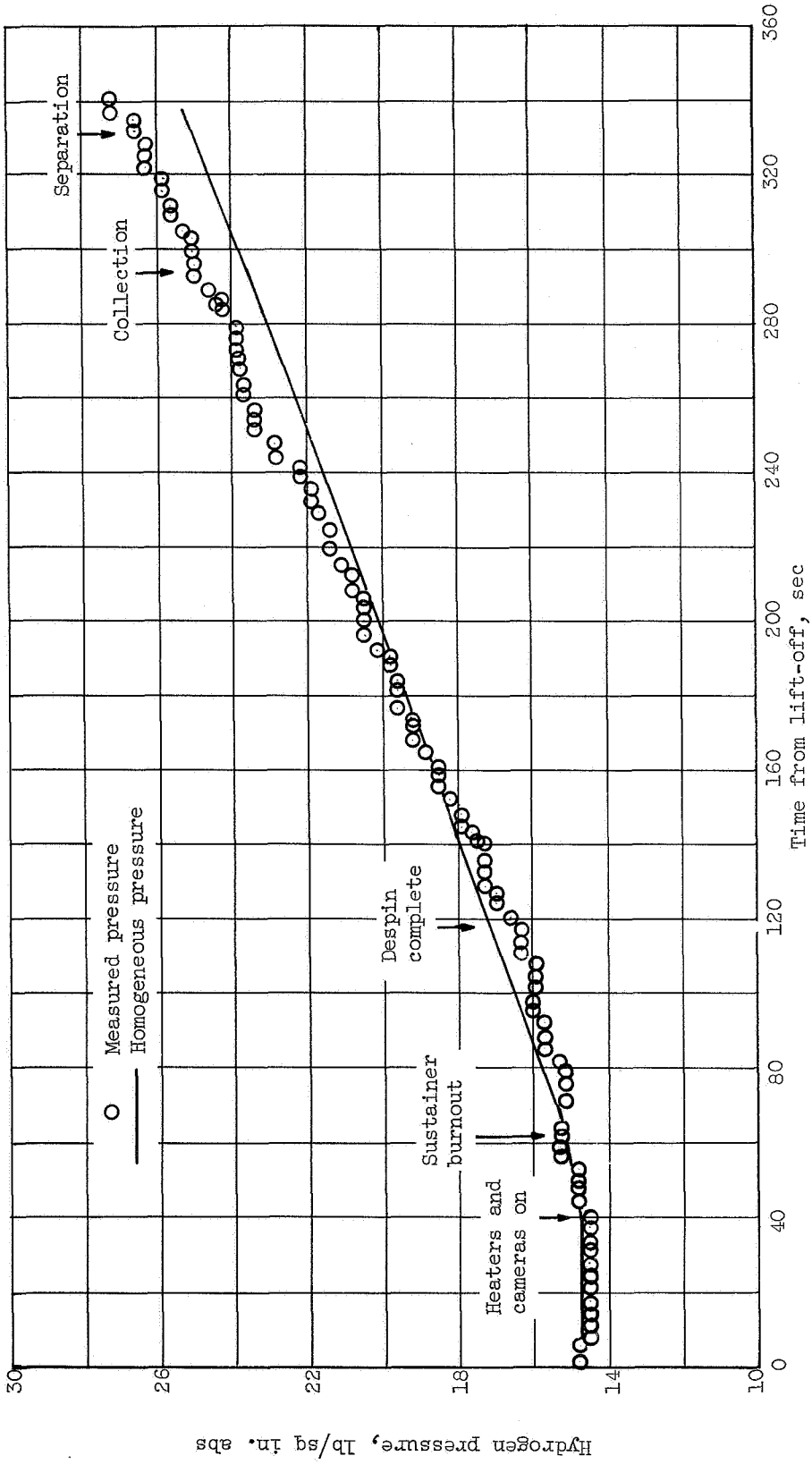

Figure 18. - Hydrogen pressure history.

CONFIDENTIAL

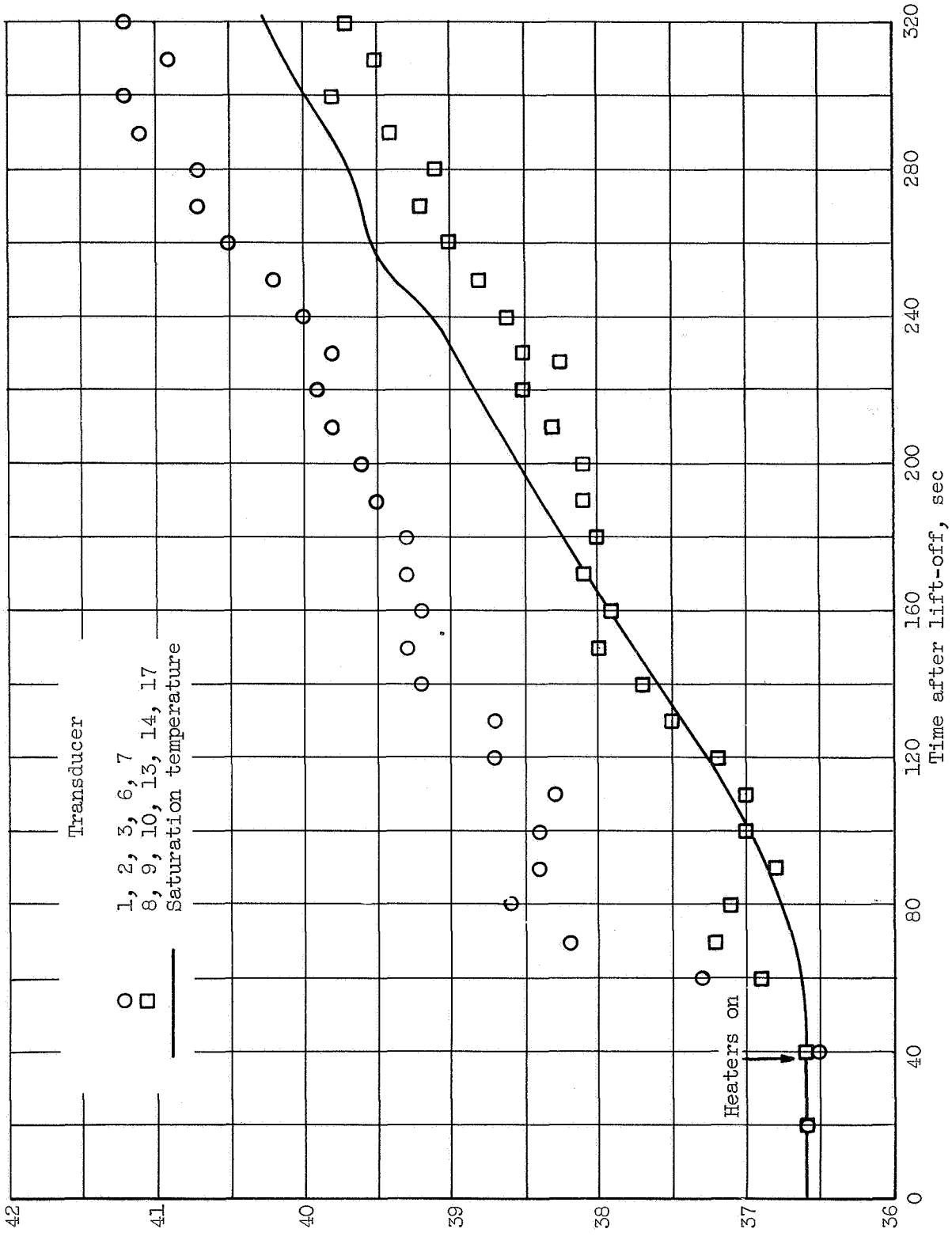

Figure 19. - Average liquid-wetted-wall temperature compared with saturation temperatures corresponding to flight pressure.

CONFIDENTIAL

CONFIDENTIAL

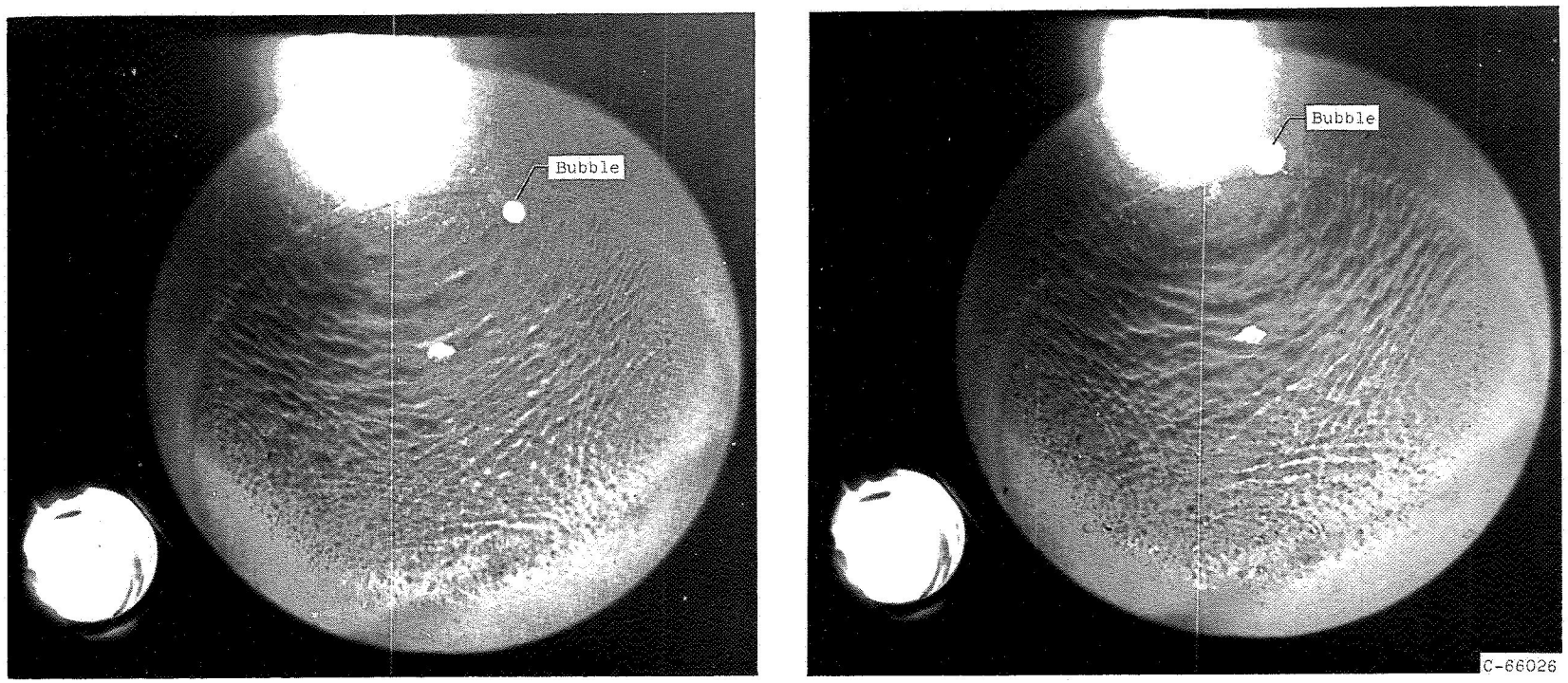

211.8 sec

212.0 sec

(a) Apparent upward and downward motion of bubble.

Figure 20. - Liquid hydrogen from 211.8 to 293.7 seconds after lift-off.

CONFIDENTIAL

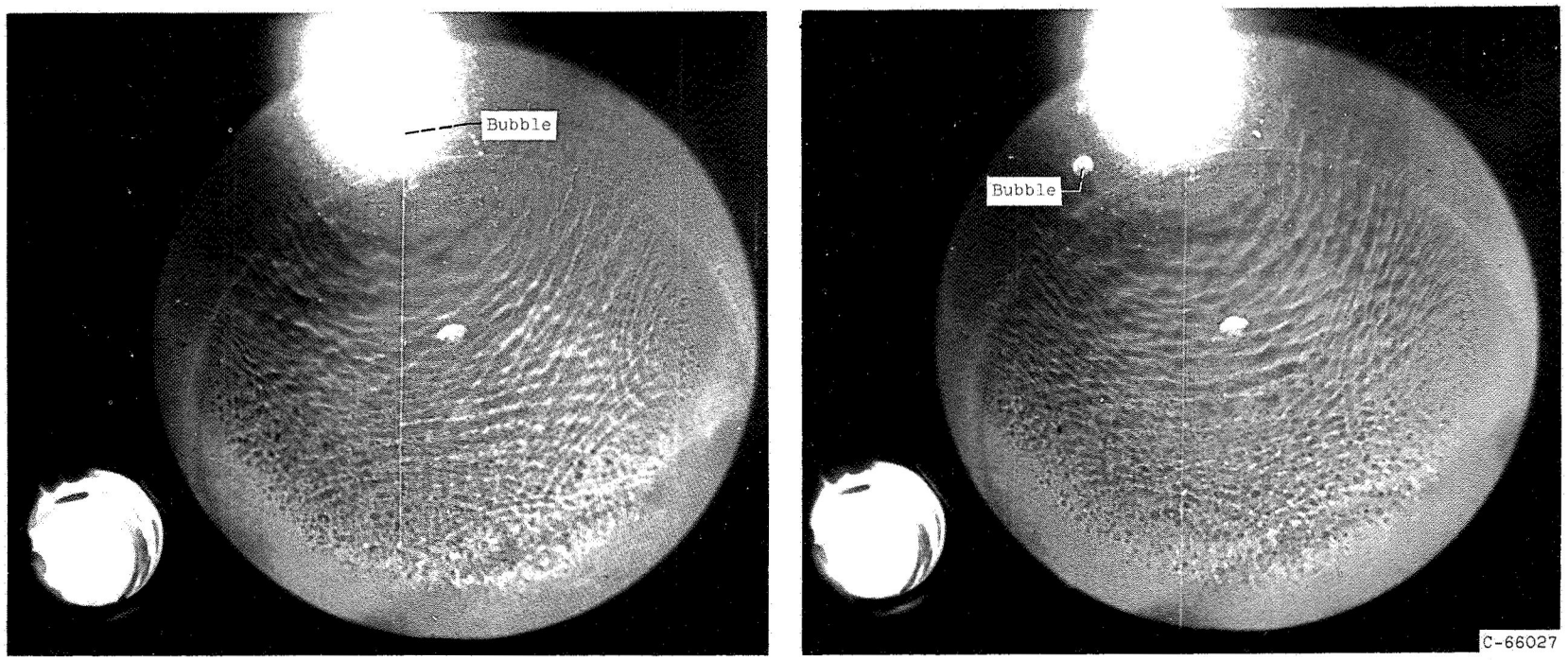

212.2 sec

212.4 sec

(a) Concluded. Apparent upward and downward motion of bubble.

Figure 20. - Liquid hydrogen from 211.8 to 293.7 seconds after lift-off.

CONFIDENTIAL

CONFIDENTIAL

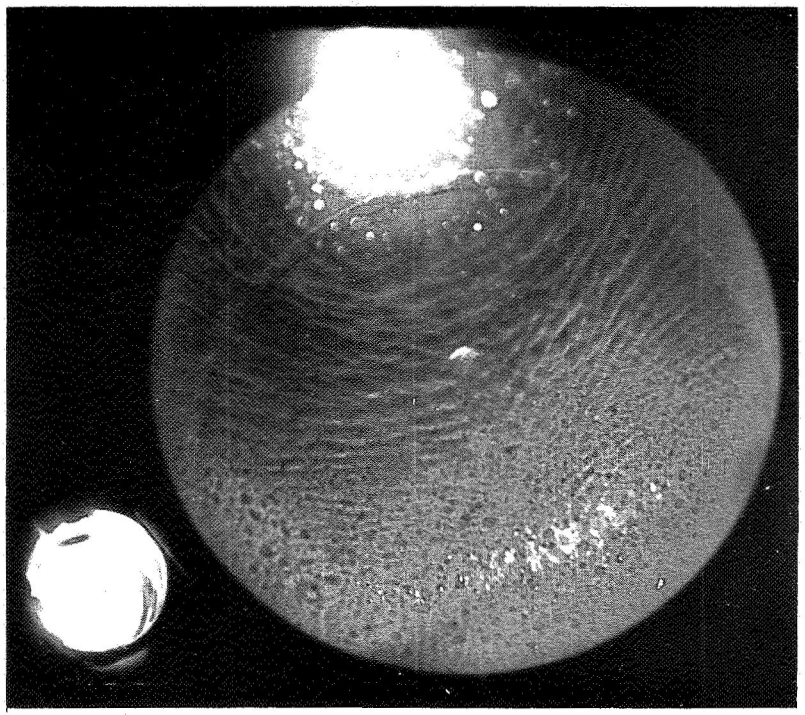

278.7 sec

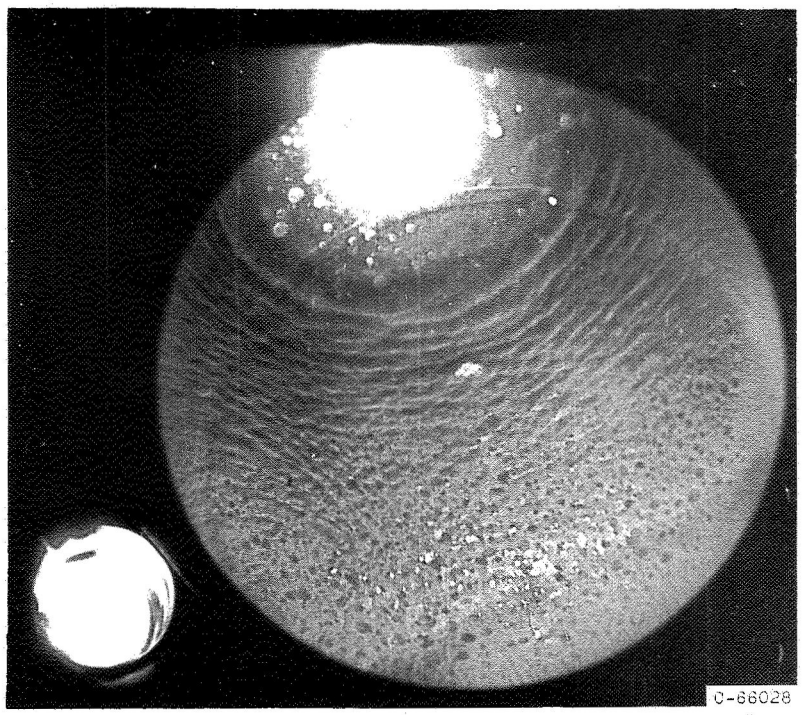

280.6 sec

CONFIDENTIAL

(b) Disturbed surface and numerous larger bubbles during latter part of weightless period.

Figure 20. - Liquid hydrogen from 211.8 to 293.7 seconds after lift-off.

CONFIDENTIAL

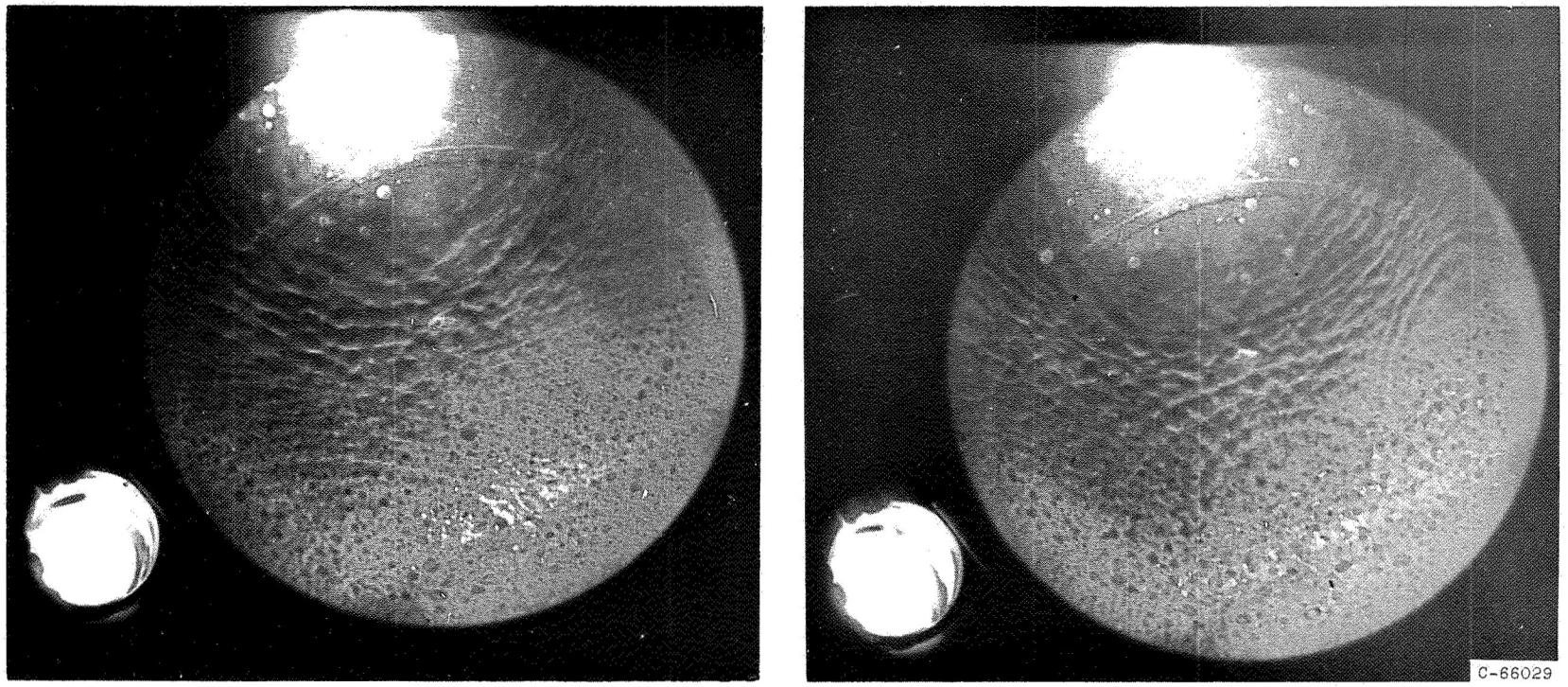

288.4 sec

293.7 sec

(b) Concluded. Disturbed surface and numerous larger bubbles during latter part of weightless period.

Figure 20. - Concluded. Liquid hydrogen from 211.8 to 293.7 seconds after lift-off.

CONFIDENTIAL

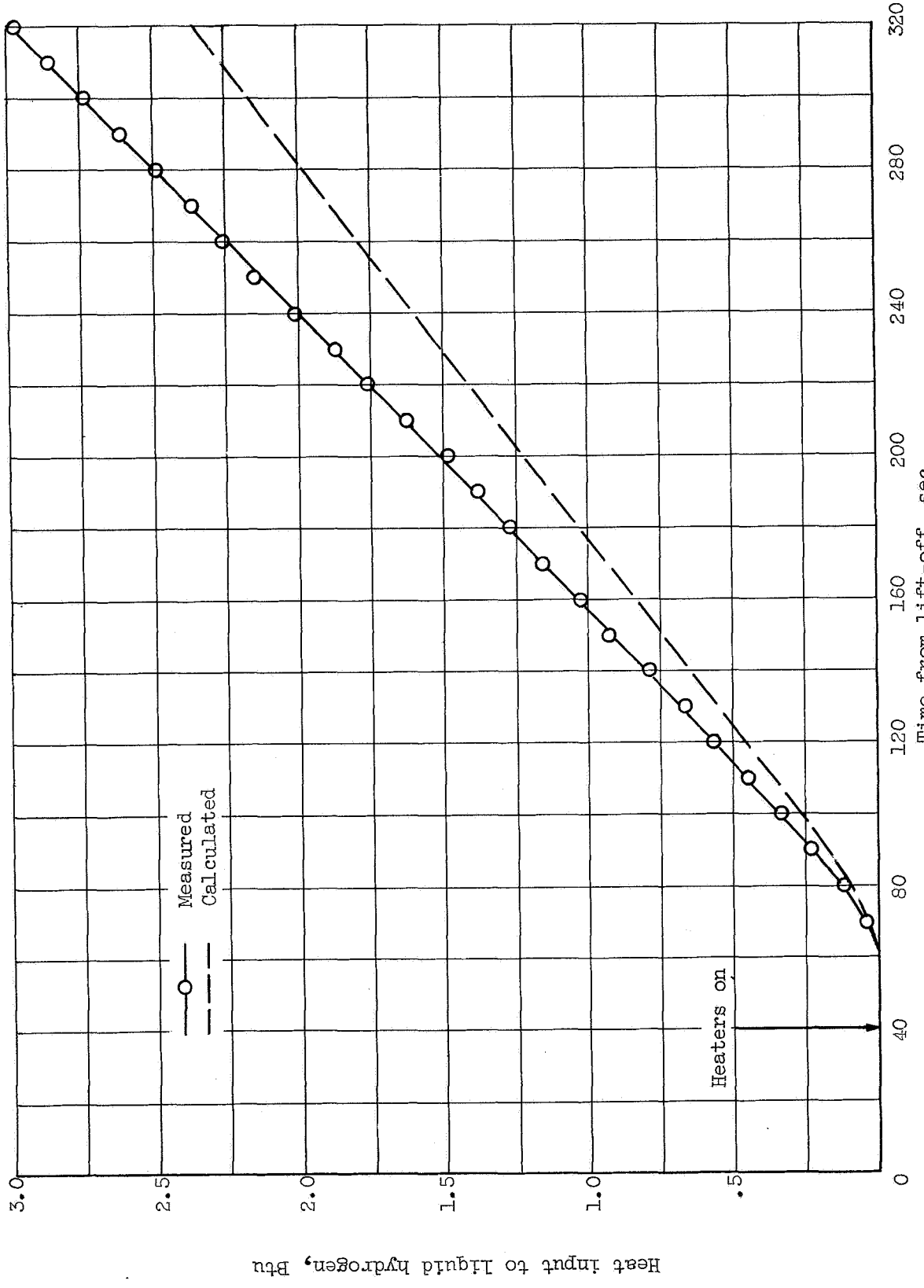

Figure 21. - Comparison of measured heat input with calculated heat input for ground test conducted with nonuniform heating and uniform mixing.